An integrated approach to define new plays in mature oil basins: the example from the Middle Magdalena Valley basin (Colombia)

P. Cabello[1], C. Lopez[2], N. Gamba[2], M. I. Dussán[2], E. Torres[2], C. I. Ballesteros-Torres[2], M. T. Cantisano[2], N. Marfisi[2], R. Calvo[1], Y. M. Vázquez-Taset[3], E. Ramos[1]

[1] Dept. Dinàmica de la Terra i de l'Oceà, Institut de Recerca Geomodels. Facultat de Ciències de la Terra, Universitat de Barcelona, c/Martí i Franquès s/n, 08028, Barcelona. pcabello@ub.edu

[2] Ecopetrol S.A., Carrera 7 No 32-13 Ed. San Martín, Piso 7, Bogotá, Colombia

[3] Escuela de Ciencias Geológicas e Ingeniería, Yachay Tech University, Hacienda San José s/n y Proyecto Yachay, San Miguel de Urcuquí, Ecuador

ACKNOWLEDGEMENTS

We are indebted to Ecopetrol S.A. for providing the dataset used and for funding this research. Thanks are due to Schlumberger for a donation of Petrel E&P licenses and for the technical support to use the software. Support from MEyC (Project SEROS CGL2014-55900-P) and Generalitat de Catalunya (2014SGR467) is gratefully acknowledged. The constructive comments and suggestions by Brian Horton and an anonymous reviewer are much appreciated and have improved the manuscript.

ABSTRACT

An integrated approach to detect new areas of potential interest associated with stratigraphic traps in mature basins is presented. The study was carried out in the Middle Magdalena Valley basin, in Colombia. The workflow integrates outcrop and subsurface interpretations of facies, activity of faults, distribution of depocenters and paleocurrents, and makes use of them to construct a 3D exploration scale geocellular facies model of the basin. The outcrop and well log sedimentological analysis distinguished facies associations of alluvial fan, overbank, floodplain and channel-fill, the last one constituting the reservoir rock. The seismic analysis showed that tectonic activity was coeval with the deposition of the productive units in the basin, and that the activity ended earlier (before the middle Miocene) along the western margin than along the eastern margin. Paleogeographic reconstructions depict transverse and longitudinal fluvial systems, alluvial fans adjacent to the active basin margins and floodplain facies dominating the structural highs and the southwest depositional limit. These reconstructions provided statistical data (lateral variograms) to construct the model. The exploration scale facies model depicts the complete structure of the basin in three dimensions, and the gross distribution of the reservoir and seal rocks. The predictive capability of the model was evaluated positively and the model was employed to detect zones of high channel-fill facies probability that form bodies that are isolated or that terminate upwards in pinch-outs or truncated by a fault. Our approach can prove helpful in improving general exploration workflows in similar settings.

INTRODUCTION

The search for yet-to-be-discovered hydrocarbons in mature provinces involves investigating subtle traps, i.e. stratigraphic traps (Carll, 1880; Levorsen, 1936), which generally render reservoirs elusive. In stratigraphic traps, the mechanism for retaining hydrocarbons is due to changes in rock type related to the stratigraphy. Stratigraphic traps have been classified (Rittenhouse, 1972; Biddle and Wielchowsky, 1994; Gordon, 1997) as: a) primary or depositional traps associated with facies changes or depositional pinchouts, and those created by buried depositional relief (e.g. carbonate reefs); b) secondary traps produced by post-depositional alteration of strata, e.g. due to diagenetic processes or to the presence of asphalt or gas hydrates; and c) associated with unconformity surfaces. Stratigraphic traps can also involve a structural component (i.e. combination trap; Levorsen, 1967), which facilitates detection. Structural trap components are linked to geometries of deformation that affect the sedimentary sequence such as faults and folds, permitting the retention of hydrocarbons.

Understanding the characteristics of the depositional environment and the structural setting of prospects under exploration proves helpful in detecting the presence of stratigraphic traps (Caldwell et al., 1997). In fluvial systems, depositional stratigraphic traps involve porous and permeable deposits normally represented by sandstone-dominated channel-fill and levee facies embedded in fine-grained impermeable floodplain deposits (Biju-Duval, 2002; Slatt, 2006). The distribution of channel-fill deposits, and hence the potential existence and formation of stratigraphic traps are controlled by the interaction of a number of factors such as the fluvial style, grain size, avulsion of channels, sedimentary rate, tectonics, base-level changes, climate and type of basin. These factors determine the global evolution of the basin and its sedimentary infill, controlling the establishment and modification of the fluvial style, the distribution of depositional subenvironments, the paleoflow trends and the development of erosional unconformities.

New discoveries in mature basins and the inherent difficulty of determining stratigraphic traps call for new exploratory ideas and techniques, and revision of existing concepts and interpretations. The investigation of stratigraphic traps has historically been addressed by sequence or seismic stratigraphy (Catuneanu, 2006; Strohmenger et al., 2006; Veeken, 2007). Other studies have already embarked upon the search for stratigraphic traps on the basis of integrating non-seismic, geological data such as basin analysis information and reservoir architecture (Atkinson et al., 2006). Currently, the detection of stratigraphic traps makes use of direct fluid indicators in seismic data such as bright spots. Seismic inversion and seismic attributes are employed to interpret rock/pore fluid properties and stratigraphic and sedimentological models (Caldwell et al., 1997; Chopra and Marfurt, 2005; Torrado et al., 2014). Stratigraphic or process-based modeling has proved useful in predicting the distribution of reservoir and seal rocks in basins (Falivene et al., 2014). This technique models accommodation, supply, and transport to simulate the filling of sedimentary basins (Granjeon, 2010), producing comprehensive pictures of basins that incorporate both structure and facies distribution (Granjeon, 1996; Koltermann and

Gorelick, 1996; Granjeon and Joseph, 1999; Granjeon, 2009, 2014; Gratacós et al., 2009; Carmona et al., 2016). Basin-scale petroleum systems models are applied in mature basins to consider migration pathways, new potential source rocks and entrapment mechanisms (Neumaier et al., 2014; Sánchez et al., 2015). Most of these techniques, however, present some limitations. In mature basins with a long productive history, seismic datasets may suffer from limited quality, low resolution or insufficient cover. This could result in the failure to detect subtle traps. Despite the advantages of stratigraphic modeling, this technique proves difficult when modeling sedimentary processes in nonmarine sedimentary basins. Moreover, the low resolution of stratigraphic and sedimentological features of basin-scale petroleum systems models render them unsuitable for detecting stratigraphic traps.

Our study, therefore, seeks to present a methodology that facilitates the detection of stratigraphic and combined structural-stratigraphic traps, enabling us to redirect new exploratory activities in mature basins. Our approach is based on the construction of a 3D exploration scale model that reproduces the main structures and the overall distribution of reservoir and seal rocks in a whole basin, integrating geological data from different sources (outcrop, seismic and wells). Part of the method is based on stochastic modeling techniques widely used at the hydrocarbon production scale. Although this can be regarded as a complement to other techniques, it is of interest because it offers an overall view of the whole basin.

The mature Middle Magdalena Valley basin, in Colombia, was selected to implement this approach. This basin has been one of the most prolific hydrocarbon provinces of the Andean Range. To date, most fields that have been discovered are located in Paleocene – middle Miocene nonmarine sandstone reservoirs, and the majority of them are related to structural traps. After decades of exploitation, most of these fields are today regarded as mature or maturing, and the main structural traps in the basin are plays already proved. In such a scenario, new finds are expected to be related to new plays associated with stratigraphic or combined structural-stratigraphic traps (Allen et al., 2006).

GEOLOGICAL SETTING

Regional geological framework

In Colombia, the Northern Andes are divided into three main NNE-trending ranges, the Western, the Central and the Eastern Cordilleras, which are separated by alternating sedimentary basins, the Magdalena Valley and the Llanos Basins (Figure 1). The Western Cordillera is considered an allochthonous oceanic terrane, predominantly Upper Cretaceous in age, accreted to the South America margin in Latest Cretaceous – earliest Paleocene times (McCourt et al., 1984; Aspden and McCourt, 1986; Aspden et al.; 1987; Cediel et al., 2003). The Central Cordillera corresponds to the Andean volcanic arc that resulted from the subduction of the oceanic Nazca Plate beneath the South America Plate. It is largely composed of low to medium-pressure metamorphic rocks intruded by Mesozoic and Cenozoic calc-alkaline plutons (Aspden and McCourt, 1986; Aspden et al., 1987; Gómez et al., 2005b). Jurassic and Cretaceous pyroclastic rocks have also been reported. The Central Cordillera forms an uplifted crustal-scale structure developed in a transpressive regime related to the oblique convergence and Western Cordillera accretion (McCourt et al., 1984; Schamel, 1991).

The Magdalena Valley Basin is a narrow, approximately north-south elongated intermontane hinterland basin that evolved in connection with the eastward advance of the Andean orogen (Gómez et al., 2005b; Horton et al., 2015; Reyes-Harker et al., 2015). Classically, it has been divided, from south to north, into the Upper, Middle and Lower Magdalena Valley Basins. Its western boundary corresponds to the Central Cordillera, where it is bounded by the Eastern Cordillera to the east. The basin contains a thick and relatively continuous sedimentary infill recording the tectonic evolution of the neighboring ranges.

The Eastern Cordillera is constituted by a continental basement made up of granulite-grade metamorphic rocks of Proterozoic to Paleozoic age. These are overlain by sedimentary to low-grade metasedimentary Paleozoic to Mesozoic rocks that are intruded by Mesozoic and Cenozoic calc-alkaline plutons (Dengo and Covey, 1993; Gómez et al., 2005b; Chew et al., 2007; Nie et al., 2010; Moreno et al., 2011). South of 7º N, the Eastern Cordillera constitutes a fold-and-thrust belt displaying opposite westward and eastward vergences that overthrusts the Magdalena Valley Basin to the west and the Llanos Basin to the east. North of 7º N, the Eastern Cordillera is divided into a north-western branch, the Santander Massif, and north-eastern branch, the Mérida Andes (Figure 1).

The Llanos Basin is a large retroarc foreland basin located eastwards of the Eastern Cordillera. Its sedimentary infill records Upper Cretaceous to Cenozoic deposition in shallow marine, transitional and continental environments, showing an increasingly nonmarine tendency towards the east. The sediment provenance for the eastern Llanos Basin was from the east, from the Guyana Shield, which constitutes the Precambrian continental basement of the northern Amazonian Craton (Cordani et al., 2000). Westwards, its sedimentary infill also contains upper Eocene – lower Miocene alluvial deposits from the Eastern Cordillera (Reyes-Harker et al., 2015).

Basin development and evolution

The present-day locations of the Magdalena Valley Basin, Eastern Cordillera and part of the Llanos Basin corresponded in the Triassic to Early Cretaceous to a rift system, which was probably attributed to the separation of North and South America (Jaillard et al., 1990; Cooper et al., 1995; Sarmiento, 2001; Spikings et al., 2015). It gave rise to local accumulations of up to 3000 m (9843 ft) of a syn-rift sequence that currently crops out in the Eastern Cordillera (Hebrard, 1985; Fabre, 1987). This sequence is made up of Triassic and Jurassic red-beds and volcaniclastic strata accumulated into subbasins fed from local igneous source areas (Horton et al., 2015). This sequence evolved upwards into shallow marine deposits in the Early Cretaceous.

Later, the area developed into a convergent margin, with oceanic subduction and formation of a volcanic arc (Central Cordillera), which promoted the subsequent accretion of oceanic terranes (Western Cordillera) to the Central Cordillera. In this convergent environment, deformation and shortening in Upper Cretaceous to lower Paleocene times led to the formation of a large foreland basin that included the present-day Magdalena Valley Basin, Eastern Cordillera and Llanos Basin areas (Van der Hammen, 1961; McCourt et al., 1984; Gómez et al., 2003, 2005a, 2005b). The earliest deposits in this basin were marine, but the Paleocene Lisama Fm. (Figure 2) provides evidence of the transition from marine to nonmarine deposits (Cooper et al., 1995; Gómez et al., 2005b; Moreno et al., 2011). This paleoenvironmental transition correlates with a shift in the sediment transport direction from northwards to eastwards (Moreno et al., 2011), and with changes in detrital zircon geochronology from Proterozoic-dominated ages, indicating Amazonian craton provenance, to Phanerozoic-dominated ages with an Andean orogene provenance (Nie et al., 2010; Moreno et al., 2011; Horton et al., 2012; Horton et al., 2015).

Further evidence of western provenance includes granitic and volcanic pebbles of the lower Maastrichtian conglomerates in the Magdalena Valley Basin derived from the Central Cordillera (Cooper et al., 1995). These variations in paleocurrents, provenance, and thermochronology of detrital zircons data have been interpreted as the onset of the uplift and exhumation of the Central Cordillera in Latest Cretaceous – Paleocene times

(Gómez et al., 2003; Villagómez and Spikings, 2013; Horton et al., 2015), and as the formation of the afore-mentioned middle Paleocene foreland system.

The tectonic deformation propagated in a north-northeastward direction due to the oblique direction of convergence (Gómez et al., 2003, 2005a, 2005b; Parra et al., 2009; Horton et al., 2015), triggering an east–west directed compression. This resulted in the tectonic inversion of the former extensional faults attributed to the Mesozoic rift that led to the onset of the Eastern Cordillera (Barrero, 1979; Cooper et al., 1995; Sarmiento, 2001; Moreno et al., 2011; Reyes-Harker et al., 2015). The uplift of the Eastern Cordillera divided the Cretaceous – Paleogene foreland basin, resulting in the generation of the intermontane hinterland Magdalena Valley Basin on the western flank and the retroarc foreland Llanos Basin on the eastern flank (Gómez et al., 2005b; Mora et al., 2006).

There is no consensus on the date of onset of the Eastern Cordillera. Gómez et al. (2005b) documented the Late Cretaceous – early Eocene uplift of the Central Cordillera and the subsequent transfer of deformation to the Eastern Cordillera. These authors also found growth strata (middle Eocene – Oligocene) to be older in the south than in the north (upper Oligocene – early middle Miocene). Nie et al. (2010) pointed out a shift in detrital zircon U-Pb ages in samples from the Middle Magdalena Valley basin that occurred between middle – late Eocene and late Oligocene, and that has been attributed to the exhumation of the Eastern Cordillera. Moreno et al. (2011) reported an inversion of the paleocurrent trend from eastwards to westwards in the Nuevo Mundo Syncline outcrops in the latest Eocene (i.e. time of deposition of the Esmeraldas Fm., Figure 2). This change in the paleoflow direction, which persisted during the Neogene, is consistent with: a) a change in the distality of the facies, which can be interpreted as the result of the Eastern Cordillera uplift; and with b) the subsequent change of the Magdalena Valley Basin from a foreland to a hinterland basin.

Parra et al. (2012), using seismic interpretations and thermochronometric data, dated shortening and deformation in some components of the present hinterland of the Eastern Cordillera in the late Paleocene – earliest Eocene. Horton et al. (2015), also based on detrital zircon U-Pb geochronology, concluded that the incipient uplift of the Eastern Cordillera took place in the latest Eocene – earliest Oligocene, which is in agreement with the multidisciplinary study by Reyes-Harker et al. (2015). Despite the disagreement on the date of onset of the Eastern Cordillera exhumation, it is widely accepted that its major uplift is probably associated with a younger middle Miocene – Pliocene deformation phase (Dengo and Covey, 1993; Mora et al., 2010; Sánchez et al., 2012).

Stratigraphy and sedimentary infill of the Middle Magdalena Valley basin

The sedimentary infill of the Middle Magdalena Valley basin (MMVB henceforth) forms a 2 – 10 km (1 – 6 miles) thick Mesozoic and Cenozoic marine and nonmarine succession deposited over a Proterozoic to lower Paleozoic basement (Cediel et al., 2003). Above the scant Jurassic syn-rift deposits, the Mesozoic sequence mainly includes sandstones, limestones and mudstones that record a generalized marine transgression. This period was followed by a marine retreat and deposition of nonmarine strata during Cenozoic times. The regional Middle Magdalena Valley Unconformity (named herein as U0) records a significant period of upper Paleocene – lower Eocene erosion (Schamel, 1991; Rolon, 2004; Gómez et al., 2003, 2005b; Horton, 2012) whose stratigraphic gap decreases towards the east. The regional unconformity divides the MMVB infill into two sequences (Figure 2). The lower sequence is made up of deformed and eroded Paleocene and older rocks. Its thickness increases towards the east, attaining 2500 m (8202 ft) at the border with the Eastern Cordillera. The overlying sequence corresponds to relatively non-deformed units, middle Eocene to Neogene in age, which onlap the unconformity. The preserved thickness of this sequence also increases towards the east, from 0 m at the boundary with the Central Cordillera in the south to 5000 m (16,404 ft) in the Eastern Cordillera foothills.

The MMVB stratigraphic subdivision in this work (Figure 2) considers the most accepted lithostratigraphic subdivision used (Morales et al., 1958; Schamel, 1991; Gómez et al., 2005b; Caballero, 2010; Caballero et al., 2010). It includes, from older to younger, the Umir, Lisama, La Paz, Esmeraldas, Mugrosa and Colorado formations, the Real Group and the Mesa Formation. Additional minor unconformities probably triggered by tectonic deformation attributed to the evolution of the Central and Eastern Cordilleras have been reported by Gómez et al. (2003, 2005b), Restrepo-Pace et al. (2004) and Parra et al. (2012). Given these unconformities, Suárez (1996) proposed a tectono-stratigraphic subdivision of the Eocene – Miocene succession of the MMVB. This author defined six tectono-stratigraphic sequences (TS1 to TS6 in figure 2) that prove useful for the subsurface stratigraphic subdivision. The three lowermost tectonosequences, TS1, TS2 and TS3, consisting of La Paz, Esmeraldas, Mugrosa and Colorado formations, constitute the subject of the present study. The formations were deposited in a fluvio-alluvial depositional environment. The fluvial sequences are the most extensive deposits and are made up of coarse detrital sediments forming channel belts interstratified within fine-grained floodplain and overbank detrital sediments (Gómez et al, 2003, 2005a, 2005b; Caballero, 2010; Caballero et al., 2010; Moreno et al, 2011; Caballero et al., 2013). Locally, thin floodplain lacustrine sequences have also been reported. The La Paz Fm. was mainly deposited by a braided fluvial system, the Esmeraldas and Mugrosa Fms. by meandering streams, and the Colorado Fm. by a mix of meandering and braided fluvial systems.

Middle Magdalena Petroleum Geology

Two petroleum systems have been recognized in the subsurface of the MMVB (Barrero et al., 2007). In the larger and the more prolific system, Paleogene fluvial sandstones and the interstratified mudstones constitute, respectively, the main reservoir and seal. In the secondary target, the fractured limestones of the Barremian-Aptian "Basal limestone Group" are the reservoir (Morales et al., 1958).

In both petroleum systems, the Cenomanian-Santonian marine shales, marls and limestones of the La Luna Fm. are considered to be the main source rock, because of its relatively high TOC values, moderate maturity and adequate burial (Cooper et al., 1995; Spickert, 2014; Veiga and Dzelalija, 2014). This formation contains kerogen type IIs, an oil-prone kerogen similar to type II, but with a high sulfur content (Ramon et al., 1997; Sarmiento, 2011). The TOC content in shales ranges between 0.67 and 6.72%, vitrinite reflectance averages about 0.6%, hydrogen indexes are 302 mgHC/gTOC, and hydrocarbon generated by thermal cracking of kerogen (S2 index) range between 5.0 and 27.0 mgHC/g rock. In line with Veiga and Dzelalija (2014), a conservative estimate of the total area where the La Luna Fm. has reached maturity in the MMVB is 1400 km^2 (540.5 mi^2). This formation underwent limited generation of hydrocarbons in the Late Cretaceous according to the 1-D model of Spickert (2014). This model is based on data from the Ecopetrol 1613 Infantas well that is located in the La Cira-Infantas paleohigh, approximately 25 km (15.5 mi) to the north of the La Luna Fm. depocenter. The most significant phase of hydrocarbon generation commenced during the Early Cenozoic as a result of the increased heat flow during the uplift of the Central Cordillera.

The middle Eocene to middle Miocene La Paz, Esmeraldas, Mugrosa and Colorado formations (Figure 2) have hosted the largest and most productive oil fields in the

MMVB, most of them with a long production history. The most frequent trapping mechanisms consists of monoclinal dipping and/or folded series affected by faults.

DATASET AND METHODS

Our study presents a multidisciplinary workflow (Figure 3) that integrates data from both outcrop (sedimentological outcrop descriptions and logs, paleocurrent data, geological maps) and the subsurface (well cores and geophysical logs, seismic 2D lines). The workflow consists of: a) a sedimentological and paleogeographic study of the productive units; and b) a 3D reconstruction of the structure of the basin and a subsequent geostatistical modeling of its sedimentary infill.

Outcrop data acquisition and analysis

Three field studies were carried out in the eastward outcropping area of the Nuevo Mundo Syncline (Figure 4). The fieldwork included the logging of eight sedimentological sections at scales 1:50 and 1:100, with a total measured thickness of more than 435 m (1427 ft). Paleocurrent measurements were taken and detailed descriptions and sketches from outcrops were obtained. This information was used to determine the geometry and dimensions of sedimentary bodies, and to provide a preliminary estimate of facies proportions. Moreover, individual lithofacies were defined in accordance with their lithology, sedimentary structures, bioturbation index and early diagenetic characteristics. Subsequently, the lithofacies were grouped into assemblages. Finally, depositional models for each stratigraphic unit under study were proposed. These models were also based on the analysis of the well data (Figure 3).

Well data analysis

The well data included logs from a selection of 94 wells distributed throughout the basin (Figure 4). The wells traverse most of the stratigraphic interval under study and the logs exhibit sufficient quality to interpret facies associations. The log responses available for the selected wells included gamma ray, resistivity and spontaneous potential. For sixteen wells of the well dataset, continuous core or core descriptions were also available. These log records were interpreted to establish facies assemblages equivalent to those distinguished in the outcrops. Using the gamma ray log, the volume of clay (Vcl) was estimated in accordance with equation 1.

$$Vcl_{(x)} = [(GR_{(x)} - GR_{(s)}) / (GR_{(cl)} - GR_{(s)})] \times 100 \quad (1)$$

where the $GR_{(x)}$ refers to the gamma ray value at the observed position in the well for which the volume of clay was calculated (i.e. $Vcl_{(x)}$). $GR_{(s)}$ corresponds to the gamma ray value equivalent to sandstones that are devoid of clayish matrix, and $GR_{(cl)}$ indicates the gamma ray value measured for clay.

When the GR log was unavailable or when it failed to calculate the volume of clay, the spontaneous potential log (SP) was used in an expression equivalent to equation (1). Some characteristic curve morphologies with a specific range of Vcl values, thicknesses and a repetitive vertical stacking were identified in the Vcl log for those wells that had cores available. These patterns are interpreted as corresponding to one of the facies associations. Moreover, this analysis was corroborated by the deep resistivity curve. The interpretation of the electric curves was compared with the sedimentological interpretation obtained from the cores. When these two interpretations did not concur, the one from the electric logs was revised. This process led to the adoption of a set of patterns that were extrapolated to the remaining wells without available cores. This was undertaken to obtain a facies association log for the complete set of wells. A final quality control of the results was performed in all the wells. The well log obtained provided an insight into the distribution of the main facies associations throughout the basin. Eight wells of the total well dataset were reserved to calibrate and validate the 3D geostatistical facies model (Figure 4).

The position in the wells of the unconformities that bound the stratigraphic units (U0, U1, U2 and U3; Figure 2) was transferred from the seismic interpretation using synthetic seismograms and a check-shot survey. Moreover, a palynologic analysis allowed us to corroborate these positions and to interpret the boundary between the La Paz and Esmeraldas formations that was not traced in the seismic lines. The biostratigraphic analysis was performed on 67 wells, using data collected during the last 15 years by Ecopetrol. The biostratigraphic setting used has been published by Reyes-Harker et al. (2015). The La Paz Fm. was associated with the *Striatpollis catatumbus* biozone and the Esmeraldas Fm. with the *Racemonocolpites facilis – Rhoipite guianensis "perbonus"* biozones. The biozones *Rhoipites guianensis – Magnastriatites grandiosus* are attributed to the Mugrosa Fm., whereas *Echitricolporites maristellae – Retitricolpites simplex* biozones to the Colorado Formation.

Seismic analysis

The seismic data include a total of 3500 km (2175 mi) of 2D lines that come from surveys obtained from different acquisition campaigns (Figure 4). The major faults and the unconformities U0, U1, U2 and U3 were interpreted in the seismic profiles. The unconformities were identified on the basis of truncation relationships and onlap and downlap terminations of the reflectors. The seismic interpretation was analyzed to infer an overall fault activity timing in the basin. This was based on cross-cutting and overlapping relationships between the stratigraphic horizons and the faults, and on the presence of growth strata.

3D modeling

The 3D exploration scale facies model was built to reproduce the occurrence of the main facies belts in the MMVB. The 3D modeling follows a conventional workflow used in reservoir modeling that includes: a) the construction of the stratigraphic and structural model; b) the construction of a 3D grid; and c) the assignment of a facies category to each grid cell by using geostatistical methods (Figure 3). A conceptual depositional model for each stratigraphic unit represented by paleogeographic reconstructions was used to define and guide the facies modeling strategy.

Construction of the 3D stratigraphic and structural framework

The stratigraphic framework of the 3D model comprises the major faults interpreted in the seismic lines, the U0, U1, U2 and U3 unconformities, the limit between the La Paz and Esmeraldas formations and the topographic surface. The interpolation of the traces interpreted in the seismic lines provided a 3D reconstruction of the surfaces in the time domain. The boundary between the La Paz and Esmeraldas formations was modeled by means of the interpolation of the positions recorded in the wells and guided by the geometry and terminations of the seismic reflectors within the tectonosequence 1. The reconstructed surfaces were converted to depth domain by using a set of linear and quadratic velocity functions derived from a check-shot survey. The final converted surfaces resulted from the average of the linear and the quadratic conversions. The topography was reconstructed using a digital terrain model with 90 m (295 ft) of resolution, supplied by NASA (i.e. NASA Shuttle Radar Topographic Mission, SRTM), which was draped with a geological map of the region. The horizons and the faults were adjusted to their positions in the wells, and to the corresponding outcropping traces. The 3D reconstruction of the structural framework allowed us to obtain true vertical thickness maps of each stratigraphic unit (Figure 3).

Construction of the 3D exploration scale facies model

The grid cells of the model were designed as regular cells of 250 m by 250 m (820 ft by 820 ft) in a horizontal plane. They were oriented following a north-northeast – south-southwest direction, which corresponds to the mean orientation of the structures. The grid layering must mimic the reflector geometries and terminations. However, within the modeling area a wide variety of configurations were recognized (i.e. onlap, truncations, growth strata, conformable strata, etc.), which complicates an accurate reproduction of each bedding feature. It was, therefore, decided to vertically subdivide the 3D volume by selecting a proportional layering for each unit (i.e. layers parallel to the base and to the top of the bounding horizons). The number of layers was established in such a way that the mean cell thickness was 3 m (10 ft). This vertical subdivision ensures sufficient resolution to adequately represent the facies associations. This resulted in a final 3D grid with 100 million cells.

The well logs with the interpretation of the facies associations were upscaled to the 3D grid, and each grid cell that was intersected by the well trajectory was assigned the dominant facies association. These rescaled logs were used to elaborate facies proportion maps (Figure 3). The remaining modeling cells of the MMVB model were populated by applying two pixel-based algorithms and by adopting a hierarchical approach (Figure 3). First, the transition from alluvial fan to fluvial deposits was modeled using a stochastic algorithm. This algorithm is based on the truncation of the sum of a deterministic linear expectation trend and a Gaussian random field (MacDonald and Aasen, 1994; Falivene et al., 2009). The trend is used to reproduce the progradational or retrogradational stacking pattern and defines the mean boundary between the sedimentary bodies. The Gaussian field reproduces the serrated geometry of the gradual facies transition. It is controlled by variograms and ensures conditioning to hard data. In the present case study, the geometry and positioning of the trend was fixed in accordance with the well data and paleogeographic reconstructions. The parameters governing the Gaussian field were determined by a trial-and-error approach until a reasonable result was obtained.

Second, the fluvial deposits were modeled using the Sequential Indicator Simulation (SIS). This algorithm is used to model the distribution of categorical variables that are expressed as a series of indicator variables, one for every category (Journel and Alabert, 1989; Gómez-Hernández and Srivastava, 1990; Deutsch and Journel, 1998). The values of the indicator variables represent the probability of a certain category occurring at a particular location (Deutsch, 2006). In the upscaled cells, probabilities are maximum (i.e. 1) or minimum (i.e. 0), whereas for the remaining unsampled locations the algorithm estimates the related probabilities using global proportions, variography, and hard data amongst other parameters. Because well spacing did not provide appropriate lateral experimental variograms, they were derived from paleogeographic maps. These maps were transformed into indicator maps and the horizontal variograms along the directions of maximum and minimum horizontal anisotropy were obtained (Table 1). The paleogeographic reconstruction of the La Paz Fm. shows a predominance of one facies association with the result that no variograms could be extracted from it. The variograms were, therefore, estimated from the facies proportion maps following the same approach. The vertical variograms were obtained from the upscaled facies association logs. The upscaled wells also provided the global facies assemblage proportions and the vertical trends that were used to constrain the modeling (Table 1 and Figure 3).

Twenty realizations of the MMVB facies association model were generated. The multiple realizations were produced to average stochastic fluctuations and to obtain representative statistics (Goovaerts, 2006). Finally, a 3D property that represents the most probable location of the reservoir facies category in the 20 realizations was obtained. To compute this response, each realization was transformed into a probability parameter in which the cells representing reservoir facies category were assigned a probability of 100%, and those representing other facies were assigned a null probability (i.e. 0%). The final 3D property representing the probability of reservoir facies occurrence in the 20 realizations was computed by averaging the 20 parameters obtained.

Evaluation of the 3D exploration scale facies model

The 3D exploration scale facies model of the MMVB was used to investigate areas associated with new stratigraphic and structural-stratigraphic traps (Figure 3). Moreover, the model was subjected to an evaluation process to validate its capacity of prediction and consistency. The model was evaluated in two ways. First, its accuracy or capacity of predicting the rock type distribution in the subsurface was estimated by a well-calibration process. Second, the ability of the model to honor the original statistics was assessed by comparing the facies proportions with the original well dataset. The well-calibration process used the eight wells reserved in the modeling process (i.e. calibration wells in Dataset and Methods section; Figure 4). The calibration process consisted in calculating the percentage of agreement between the calibration wells and the 3D channel-fill probability parameter (i.e. average of the 20 realizations of the facies model). To this end, the probability parameter was transformed into an indicator parameter by assigning value 1 to those cells with probabilities equal to or higher than 50%, and value 0 to the remaining cells. Subsequently, the indicator parameter was transferred to the calibration wells and a new log was generated and compared with the original facies log.

RESULTS

Facies analysis

Eighteen individual lithofacies were defined in the outcrops and were divided into four main groups on the basis of their dominant lithology: gravely (G), sandy (S), sandy silty

(SM) and silty (M) lithofacies. Table 2 contains a description and interpretation of these lithofacies. The lithofacies were grouped into four assemblages or facies associations referred to as A (alluvial fan deposits), C (channel-fill deposits), O (overbank deposits), and F (floodplain deposits).

Facies association A (alluvial fan deposits)

Facies association A is primarily characterized in outcrop by lithofacies SMm, SMmd and SMmr, with facies Sm, Smb, Sr and St as subordinate elements (Table 2). Generally, the lithofacies are not vertically arranged, but form thick monotonous successions of fine-grained sediment with floating granules and pebbles and superposed diagenetic and biological features (Figure 5a and 6a-c). The subordinate sandy lithofacies, however, form isolated fining- and thinning-upwards sequences that are 1 to 1.5 m (3.3 to 4.9 ft) thick (Figure 6e). In outcrop, facies association A was only identified in the Mugrosa Fm., where it is dominant (Figure 7).

In the well logs, a distinctive Vcl pattern of facies association A was not identified. Of the available cores, only those close to the NW sector showed this facies association. It is made up of massive, matrix-supported breccias with poorly-sorted angular clasts, and forms unsaturated oil intervals (Figure 5b). Facies association A was identified in the cores of the La Paz and Esmeraldas formations, and represents 7.8% and 1.8%, respectively, of the global facies proportions in the wells (Table 1).

The dominant matrix-supported sandstones (facies SM) are interpreted to have resulted from deposition by unconfined mud flows in a middle to distal part of an alluvial fan (Figure 6k) where the sandy fining- and thinning-upwards sequences represent deposits associated with the distributary stream channels. In areas of the alluvial fan that underwent long periods of non-sedimentation, vegetation proliferated, modifying the former deposits by soil-forming processes. The matrix-supported breccias recognized in the subsurface are interpreted as massive, unconfined debris flows attributed to a proximal alluvial fan environment (Figure 6k).

Facies association C (channel-fill deposits)

In outcrop, facies association C comprises lithofacies Gm, Sm, Sp, Sh, Sr and St with facies Gp, Sm, Smb and Sh as subordinate elements (Table 2). These lithofacies are arranged in fining- and thinning-upwards sequences, which are usually 1 to 2 m (3.3 to 6.6 ft) thick and have slightly erosive basal surfaces (Figures 6d and 6e). Generally, they appear vertically stacked (Figure 5c), forming packages that reach up to 119 m (390.4 ft) in thickness in the La Paz Fm., and 27 m (88.6 ft), 10 m (32.8 ft) and 11 m (36 ft) in the Esmeraldas, Mugrosa and Colorado formations, respectively. Facies association C is largely composed of clean unbioturbated sandstones with good reservoir properties. It is present in a proportion that ranges from 100% in the outcrops of the La Paz Fm. to 21% in the outcrops of the Mugrosa Fm. (Figure 7).

In the well logs, the corresponding Vcl curve exhibits a blocky-like expression, forming vertical sequences with minimum thicknesses of 3 m (10 ft). Vcl values are equal to or below 40%, and show an upwards increasing trend. In core, facies association C is made up of fining-upwards sandstone-dominated intervals with a grain size ranging from very coarse to very fine, and which contains subordinate subrounded to subangular clast-supported conglomerates (Figures 5d and e). The sandstones commonly display large and small-scale cross lamination. Internal erosional surfaces are identified either by an abrupt increase in grain size or by the presence of mud-clast horizons. In core, this facies association is saturated with oil. Facies association C represents 55.5%, 38.5%, 36.8% and 35.9% of the global proportions in the wells (Table 1) for the La Paz, Esmeraldas, Mugrosa and Colorado formations, respectively.

Facies association C is interpreted as the result of the migration of different types of large and small-scale bed forms in fluvial channels. The erosional surfaces are associated with channel reactivation events. There exists some uncertainty in the interpretation of the fluvial style. Facies association C can be attributed to bars and sand waves in a braided system or to the result of the migration of point bars in a meandering fluvial system (Figures 6l and 6m). Lateral accretion surfaces identified in outcrops belonging to the Esmeraldas and Colorado formations are interpreted as lateral migration of channels in meandering fluvial systems (Figure 5c). However, because of the restricted lateral extent of most of the outcrops, it was not always possible to find diagnostic criteria to confirm the fluvial style.

Facies association O (overbank deposits)

In outcrop, facies association O is constituted by lithofacies Sm, Sr, S/M, Ml and MSl, with facies, Smb, Sh and Mm as subordinate elements (Table 2). It is arranged in 1 to 2 m (3.3 ft to 6.6 ft) thick, coarsening- and thickening-upwards sequences (Figures 5f and 6f). The lower portions of the sequences are laminated or massive, whereas the upper and coarser parts frequently exhibit tractive structures and reactivation surfaces. Occasionally, a thin channel-fill sequence with the upper surface affected by bioturbation or mud cracks is identified at the top. The sequences usually appear isolated, although they have sometimes been reported to form packages of up to 5 m thick (16.4 ft) consisting of three vertically stacked sequences. Facies association O was rare in the Mugrosa Fm. and in the lower part of the Colorado Fm. (Figure 7).

In the Vcl logs, overbank deposits were identified as packages with thicknesses below 3 m (10 ft) showing a serrated shape and a variable range of values. In core, this facies association was identified as an alternation of mudstone and sandstone thin beds, with sharp bases and decimetric thicknesses arranged in coarsening-upwards sequences.

Sandstones vary in grain size from very fine to very coarse and occasionally contain few conglomerates. They are moderate to well sorted, and show parallel and wavy lamination. *Palaeophycus*, *Skolithos* and *Planolites* trace fossils are also characteristic of these intervals. In core, facies association O is occasionally saturated with oil. This facies association represents 8.3%, 14.7%, 16.1% and 15.6% of the global proportions in the wells for the La Paz, Esmeraldas, Mugrosa and Colorado formations, respectively (Table 1).

Facies association O is interpreted as the progradation of crevasse splays from the fluvial channels to the floodplain (Figure 6m). The sandstone percentage varies depending on the position of the outcrop with respect to the feeding channel. In a proximal location, the sequence is more complete and sandy, similar to the sequence represented in figure 6f, whereas, in a more distal location, the sequence is limited to the muddy Ml and Mm facies.

Facies association F (floodplain deposits)

In outcrop, facies association F is primarily made up of lithofacies Mm, Mmd, Mmr Mmn and Ml, with facies MSl as a subordinate element (Table 2). This facies association lacks a clear sequential arrangement, and is characterized by relatively monotonous successions of fine-grained deposits with ample evidence of bioturbation and edaphic processes. In accordance with the intensity of these overprinted diagenetic or biological processes, facies association F was divided into four subtypes (Figure 6g-j) that represent the deposition in specific subenvironments. Facies association F was identified in the Esmeraldas and Colorado formations (Figure 5g), but not in the outcrops of the La Paz and Mugrosa formations (Figure 7). In the Esmeraldas Fm., it consists of intervals of 1.5 to 2 m (4.9 to 6.6 ft) in thickness, and in the Colorado Fm., this facies association is up to 38 m (124.7 ft) thick.

In the well logs, it was identified by Vcl values equal to or higher than 75%, forming packages of varying thickness. In core, these deposits are associated with reddish to greenish, massive mudstones, occasionally containing some fine-grained sandstones. Densely bioturbated intervals exhibit traces of *Scoyenia*, and to a lesser extent, of *Paleophycus and Skolithos*. These intervals were associated with the incipient development of paleosols. *Planolites* traces were also recognized. In core, this facies association is not saturated with oil. It represents 28.4%, 45.0%, 47.1% and 48.5% of the global proportions in the wells for the La Paz, Esmeraldas, Mugrosa and Colorado formations, respectively (Table 1).

This facies association is interpreted as the deposition of fine-grained sediment in the floodplain by unconfined flows during channel overflow (Figures 6k, 6l and 6m). However, subaerial conditions prevailed in the floodplain between these flooding episodes.

Fault activity

The major faults interpreted in the seismic lines are NE – SW to N – S oriented and correspond to thrusts and faults with a reverse component in displacement. In general, it was observed that the tectonic activity ended earlier (i.e. before middle Miocene) along the western margin (Central Cordillera) than along the eastern margin of the basin (Eastern Cordillera) (Figure 8). This interpretation is consistent with the eastwards displacement of the deformation of the Andean orogen (Gómez et al., 2005b; Parra et al., 2009; Horton et al., 2010; Nie et al., 2010).

Along the western margin, the Cantagallo, Cantagallo Este and Llanito faults were active in the middle Eocene during the deposition of the La Paz and Esmeraldas formations. The Colorado Fm. fossilized the Cantagallo system (Figure 9a), whereas the Llanito fault activity ceased before the deposition of the Mugrosa Formation. In the north-central sector, the activity of the Sogamoso fault was coeval with the sedimentation of the Esmeraldas and Mugrosa formations, whereas towards the north, the Llanito Reforma fault only affected the deposition of the Mugrosa Formation. In the center of the basin, the Casabe and Infantas faults were active during the deposition of the Esmeraldas, Mugrosa and Colorado formations (late Eocene to middle Miocene).

In the eastern margin, the activity of the southern structures (i.e. Mugrosa and Colorado system faults) commenced in the upper Eocene and ceased during the deposition of the Colorado Formation. However, towards the north-eastern sector (i.e. the Provincia, Peña de Oro and Santa Helena structures), the tectonic activity was mainly coeval with the deposition of the Mugrosa and the Colorado formations, indicating that the deformation started in Oligocene times, after deposition of the tectonosequence 1 and continued in the Neogene. This is evidenced by the growth strata in the Provincia anticline area (Figure 9b), also reported by Gómez et al. (2005b). This study also concluded that the initial deformation of the Eastern Cordillera foothills along the MMVB was older in the south than in the north. The interpretations of the deformation evolution in the eastern margin are also consistent with the latest Eocence-earliest Oligocene incipient uplift and exhumation of the Eastern Cordillera and with the ongoing exhumation of the Eastern Cordillera hinterland during the middle Miocene (Horton et al., 2015 and Reyes-Harker et al., 2015). No clear evidence indicating that La Salina, Guariquies and Arrugas faults controlled the sedimentation of the formations under study in the MMVB was found.

3D exploration scale model

The MMVB model reproduces the structure of the basin together with the gross distribution of the reservoir rocks (channel-fill deposits) and the seal rocks in three dimensions (Figure 10).

In the modeling area, the La Paz Fm. is interpreted to be exclusively present in the northwestern sector (Figures 10b, f and 11a). However, as reported in earlier publications (e.g. Caballero, 2010; Caballero et al., 2010; Horton et al., 2015; Reyes-Harker et al., 2015) and in the present work, the sediments of the La Paz Fm. were also deposited in the Nuevo Mundo syncline sector, which falls outside the scope of our model (Figure 4). This unit attains a maximum vertical thickness of 488 m (1600 ft), between the Cantagallo and the Cantagallo Este faults. The Esmeraldas Fm. extended over the La Paz Fm. almost over all the modeling area (Figures 10c, f and 11b), which agrees with the interpretation by Gómez et al. (2005b). Maximum vertical thicknesses are mainly concentrated towards the east, attaining 1585 m (5200 ft) opposite the Provincia structure, and to the south, in the footwall of the Colorado and Infantas faults. The southwestern margin corresponds to a depositional limit (Gómez et al., 2005b), where the Esmeraldas Fm. onlaps the U0 basal unconformity. The largest vertical thicknesses of the Mugrosa and Colorado Fms. are distributed along the eastern basin margin, where maximum values of 1645 m (5400 ft) and 1830 m (6000 ft), respectively, are observed (Figures 10d to f, and 11c and d). Their thicknesses decrease gradually towards the west and the southwest, where the units also onlap the U0 unconformity. A thinning associated with the La Cira-Infantas paleohigh located in the northwestern part of the Infantas fault is observed in both units.

The facies proportion maps obtained from the upscaled well logs show that that zones with the highest proportions of channel-fill reservoir facies do not correlate consistently with sectors of maximum vertical thicknesses of the stratigraphic units (Figure 12). However, these zones are often aligned with the structures that were active during the sedimentation. The map of the La Paz Fm. shows that the channel-fill facies association dominates the central zone of the area where the unit was interpreted (Figure 12a). The highest channel-fill proportions for the Esmeraldas Fm. are mainly found in the northwestern sector and along the eastern margin in the northern half of the basin (Figure 12b). In the maps of the Mugrosa and Colorado formations, the highest proportions are mainly located in the central, northeastern and southeastern sectors (Figures 12c and d).

The MMVB facies models shows that the channel-fill facies association form large geological bodies that can extend laterally several tens of km and that have variable thicknesses, from some meters to tens of meters (Figure 10g and 13). These geological bodies interfinger with floodplain and overbank deposits and with the alluvial fans in the basin margins (Figures 12g and 13). The channel-fill reservoir facies association in the model accounts for 55.5%, 37.4%, 35.1% and 34.8% of the volume of the La Paz, Esmeraldas, Mugrosa and Colorado formations.

The 3D channel-fill facies probability parameter shows maximum (100%) or minimum (0%) probabilities in the well positions, i.e. channel-fill facies is either present or absent in the wells (Figure 13). This is because the upscaled well logs are hard data honored by all realizations, i.e. they do not change from one realization to another. In the remaining cells, high probability sectors that contrast with low probability zones were also identified. These sectors could constitute zones of interest for investigating potential new plays.

DISCUSSION

This section includes a discussion of the evolution of the depositional systems in the MMVB and of the 3D exploration scale facies model. First, depositional models that are representative of each stratigraphic unit and that document the vertical evolution of the fluvial style in the basin are presented. Then, paleogeographic reconstructions enable us to address the areal distribution of the depositional systems with respect to the tectonic evolution of the basin. Finally, the accuracy and consistency of 3D exploration scale facies model are evaluated and some examples of new plays detected in the model are presented.

Evolution of the depositional systems in the MMVB

Depositional models

The base of the La Paz Fm. comprises a thin, discontinuous conglomeratic interval leveling the topographic lows of the paleorelief related to the basal unconformity U0. In the outcropping intervals, the unit is mainly constituted by sequences of channel infill in its lower and upper parts, whereas its middle portion is dominated by overbank deposits with subordinate channel sequences (Figure 7). Paleocurrents measured in the outcrops show two trends: the large-scale structures are arranged in an approximate north-south direction, and the small-scale structures, despite a wide dispersion, show a predominant east to northeast direction of transport (Figure 7). The dominant facies assemblage of the whole unit in the subsurface corresponds to the channel-fill deposits (Table 1), whose mean proportion does not record a recognizable vertical increasing or decreasing pattern. The lower and upper parts of the La Paz Formation are interpreted as having been deposited in a braided fluvial system, where large-scale bedforms transporting coarse detrital sediment were dominant (Figure 6l). The presence of overbank deposits interstratified within channel-fill sequences in the middle part is interpreted as an increase in the avulsion processes, suggesting a higher sinuosity of the fluvial style (figure 6m). Alluvial fan deposits were identified throughout the logs of the La Paz Fm. (Figure 6k), except for the upper part.

In the eastern flank of the Nuevo Mundo syncline (outcrop 4; Figures 4 and 7), the Esmeraldas Fm. is mainly made up of channel-fill sequences with lateral accretion surfaces (Figure 5c) although the recorded outcropping percentages of overbank and floodplain deposits are low. Paleocurrent measurements for this unit show a wide dispersion (Figure 7). Like the La Paz Fm., the Esmeraldas Fm. displays two trends of paleocurrents with large-scale structures aligned in a north-south direction and small-scale structures that show a wide dispersion but with a predominant north-northeast direction of transport (Figure 7). This suggests that the Esmeraldas Fm. is the result of detrital deposition in a fluvial system with channels that display some sinuosity, and where avulsion of fluvial streams and episodic flooding occur (Figure 6m). Well data reveal that the floodplain deposits (F) are dominant in the subsurface, whereas channel-fill and overbank deposits are represented by a mean percentage of 38.5% and 14.7 %, respectively (Table 1). Since alluvial fan facies were also recognized in the cores from the northwest, the sedimentary model in figure 6k is also representative of this formation in this sector.

In outcrops 5 and 6 (Figure 4), the Mugrosa Fm. is dominated by middle to distal alluvial fan sequences (Figure 7). However, this facies association is absent in the uppermost portion of the unit in outcrop 7, which represents the transition with the Colorado Formation (Figure 7). Channel-fill deposits are present in outcrops 5, 6 and 7 and overbank deposits were only identified in outcrop 6, in a very low proportion. The Mugrosa Fm. in the studied outcrops is interpreted as a detrital deposition from unconfined mud-rich flows in the middle to distal parts of an alluvial fan system, where locally small-scale distributary channels developed (figure 6k). Nevertheless, only channel-fill, overbank and floodplain deposits were recognized in the interpreted facies association well log. They represent mean percentages of 36.8%, 16.1% and 47.1%, respectively (Table 1), suggesting that in the subsurface, the Mugrosa fluvial system is constituted by fluvial streams with some sinuosity (Figure 6m).

In outcrop 8 (Figure 4), the Colorado Fm. is mainly composed of floodplain deposits and channel-fill sequences, with a moderate contribution of overbank deposits (Figure 7).

Channel-fill sequences display lateral accretion surfaces. In its basal part in outcrop 7, the formation consists exclusively of floodplain deposits. Alluvial fan deposits were not recognized for the Colorado Formation. Subsurface data record percentages of 35.9%, 15.6% and 48.5% for channel-fill, overbank and floodplain deposits, respectively, and a slight decreasing upwards trend for the proportions of the channel-fill facies. Outcrop-measured paleocurrent data in the Colorado Fm. mainly consist of scour axes in outcrop 8 that are scarce and show a predominant west-northwest – east-southeast direction. The few small-scale sedimentary structures measured indicate a sediment transport towards the west-northwest (Figure 7). The Colorado Fm. is interpreted to have been deposited by a highly sinuous fluvial system (Figure 7m).

Paleogeographic evolution

The paleogeographic reconstructions integrate the facies proportion maps (Figure 12), fault activity (Figure 8), sedimentological analysis, paleocurrent data from outcrops and earlier subsurface studies (Aguiar and Reyes, 1982; Gómez et al., 2005a; Caballero et al., 2010, 2013) (Figure 7), and vertical thickness maps (Figure 11). The reconstructions (Figure 14) show a simplified paleogeographical distribution of the dominant facies belts (i.e. alluvial deposits, fluvial channel belts and floodplain) throughout the modeling area of the MMVB from the La Paz to Colorado formations.

The paleogeographic reconstructions proposed for the La Paz Fm. (middle Eocene) and the Esmeraldas Fm. (late Eocene) show channel-fill facies belts representing low sinuosity and high sinuosity fluvial stream deposits, respectively (Figure 14a and b). They were coeval with the alluvial fans adjacent to the northwestern margin that developed in association with the activity of the Cantagallo and Cantagallo Este faults, as described by Suárez (1996). They represent alluvial depositional systems with a main source area located in the western margin (Nie et al., 2010; Sánchez et al., 2012; Horton et al., 2015).

This interpretation is consistent with the transverse-dominated deposystems with a provenance area in the Central Cordillera interpreted by Horton et al. (2015), and is also in line with the uplift and exhumation of the Central Cordillera proposed for the latest Cretaceous-Paleocene (Gómez et al., 2003; Nie et al., 2010; Villagómez and Spikings, 2013; Reyes-Harker et al., 2015). Reyes-Harker et al. (2015) interpreted the middle Eocene of the MMVB as a period of tectonic quiescence or potential slower shortening rates in the basin. At that time, the northern connection of the MMVB with the Caribbean Sea was opened (Gómez et al., 2005b; Horton et al., 2015; Reyes-Harker et al., 2015), which is consistent with the flow of the fluvial deposystems towards the north-northeast represented in the paleogeographic reconstruction for the La Paz Fm. (Figure 14a).

The late Eocene time marks the onset of the earliest Eastern Cordillera uplift (Nie et al., 2010; Horton et al., 2015; Reyes-Harker et al., 2015; results of this work; Figure 8), which has also been interpreted as a period of a northern closure of the basin (Horton et al., 2015; Reyes-Harker et al., 2015). Accordingly, the paleogeographic reconstruction for the Esmeraldas Fm. shows potential connections of the fluvial channel belts towards the eastern and northeastern regions (i.e. the Eastern Cordillera). In this unit, floodplain deposits were dominant in the southwestern depositional limit of the unit and in elevated areas, e.g. in the La Cira-Infantas paleohigh and in the north-central zone corresponding to the northern termination of the Sogamoso and Casabe faults.

Fluvial channel belts representing high-sinuosity meandering rivers were interpreted for the Mugrosa and Colorado formations (Figures 14c and d). They are locally connected with the western margin, which would be in agreement with a transverse configuration of the depositional systems proposed by Horton et al. (2015). However, the tectonic structures in the eastern margin were already active in the Oligocene (Nie et al., 2010; Saylor et al., 2011; Sánchez et al., 2012; Reyes-Harker et al., 2015; and the results in the present work) (Figure 8). Moreover, the source area at this time was principally located in the Eastern Cordillera (Nie et al., 2010; Sánchez et al., 2012; Caballero et al., 2013; Horton et al., 2015) corresponding to the Cretaceous section (Horton et at., 2010). Furthermore, paleocurrents in the Nuevo Mundo syncline reported paleoflow with a persistent westwards component for the Mugrosa and Colorado formations (Caballero et al., 2013; and data in Figure 7). Therefore, a dominant longitudinal component of the fluvial systems reflecting paleoflow deflection of sediments from the adjacent Cordilleras is interpreted for Oligocene–middle Miocene times. With regard to the Mugrosa Fm., the incursion of alluvial fans from the central-eastern margin of the basin represents the distal alluvial fan deposits identified in the outcrops with a source area located in the Eastern Cordillera (Figures 5a and 7). Floodplain deposits dominate the northwestern and southwestern sectors, and the zone of the La Cira-Infantas paleohigh.

Evaluation and applicability of the 3D exploration scale facies model

The large geological bodies captured in the 3D exploration scale facies model reproduce the heterogeneity represented in the paleogeographic reconstructions and in the wells. The search for depositional traps associated with facies changes or depositional pinchouts of channel-fill deposits can be addressed by a visual inspection of the 3D facies model and, more effectively, of the 3D channel-fill probability parameter that averaged the 20 realizations of the facies model (Figures 10h and 13). The areas of potential interest must contain zones of high probability of channel-fill facies that form bodies that must be isolated or terminate upwards in pinch-outs or truncations with faults. Some examples of these zones are given below.

Figure 15a shows a portion of the 3D model in which some pinch-outs are detected. Channel-fill deposits are predominant in Well A, whereas they are almost absent in Well B. The pinch-outs are updip, terminating between the two wells. This could constitute a potential trap. Figure 15b also shows an updip termination of channel-fill deposits of the La Paz Formation. The 3D probability parameter reveals that this termination is potentially sealed by fine-grained facies of the overlying Esmeraldas Formation. The example in Figure 15c shows that the potential reservoir would be located in the Colorado Formation. The seal rock would be fine-grained facies of the Mugrosa Formation in the hanging wall of the fault located towards the WNW. In this case, the trap is both structural and stratigraphic. Other examples of this type of combined traps were identified in the model and should be taken into consideration.

New studies and exploratory efforts (e.g. the acquisition of new seismic survey, drilling new wells) may be subsequently developed in these or in other areas with potential interest identified in the 3D geological model of the MMVB. Furthermore, a refinement of the 3D geostatistical facies model (e.g. rebuilding of the 3D grid), and the construction of subsequent petrophysical modeling in these zones are also recommended. This would contribute more detail to the models and the predictions derived. It would also prove helpful in capturing onlap terminations or truncations that would act as potential stratigraphic traps and that could not be modeled at exploration scale.

The method applied for the construction of the geostatistical facies model in the MMVB is not a new technique in the sense that it follows the reservoir modeling workflow normally applied in the oil industry. In fact, earlier studies in the area have already dealt with geostatistical facies models. In this type of study, the modeling area corresponds to that of the production fields. The models are focused on capturing the geological heterogeneity associated with sedimentary bodies at meter scale (i.e. macroscopic scale according to Tyler and Findley, 1991), and usually make use of dense well datasets. These models are employed to predict reservoir connectivity, estimate reserves, and design and optimize production strategies. For example, the work by Gómez and Morales (2008) presents a geostatistical object-based facies model for the Oligocene – Miocene fluvial deposits for a field in the eastern margin of the basin. By contrast, our model was constructed at exploration scale and extends approximately 10,000 km^2 (3861 mi^2). It captures the large-scale sedimentary heterogeneities associated with the main facies belts represented in the paleogeographic reconstructions. In a recent article by Seyfang et al. (2017), the authors implemented a 3D geostatistical facies modeling approach to optimize the search for hydrocarbon reserves during the exploration phase. Apart from the detection of potential new plays, 3D exploration scale geostatistical facies models, such as the one in the present article, could also be used in the basin-scale petroleum systems modeling workflow to introduce a refinement in the 3D rock property distribution, which may affect hydrocarbon migration and entrapment. This workflow has been recently implemented by using process-based models in place of geostatistical facies models (Liu et al., 2016).

The success of the MMVB exploration facies model as a predictive tool (and hence, the reliability of the zones of potential interest detected) was evaluated by the well-calibration process (Figure 16). The results showed a mean positive correlation between the model and the calibration wells of 62.2%. The maximum correlation value obtained was greater than 80%, and the minimum was 49.2%, which was the only case in which the correlation was below 50%. These results validate the capacity of the model to satisfactorily predict the reservoir facies distribution in the MMVB.

In terms of facies proportions, the model slightly underestimates the channel-fill proportions recorded in the wells by less than 4% for the Esmeraldas, Mugrosa and Colorado formations. For the La Paz Fm., it overestimates the channel-fill proportions by 7%. These small discrepancies would indicate that the modeling data used are capable of honoring the original statistics. The slightly larger difference in the La Paz Formation may be attributed to the uncertainty in the estimation of the horizontal variograms. In this case, the variograms were extracted from the facies proportion maps unlike the variograms used for the Esmeraldas, Mugrosa and Colorado formations that were derived from the paleogeographic maps. The paleogeographic reconstructions, therefore, prove to be suitable for obtaining statistical parameters that describe the lateral continuity of facies distribution. This is advantageous in cases where the well data are not sufficiently dense, which occurs in the subsurface at exploration scale.

CONCLUDING REMARKS

1. An integrated approach to detect new areas of potential interest associated with stratigraphic or combined stratigraphic-structural traps in mature basins was developed. It is a comprehensive workflow that integrates outcrop and subsurface interpretations of tectonic structures and depositional environments. This workflow makes use of these interpretations to construct a 3D exploration scale facies model of the mature basin that can be analyzed and investigated.

2. The workflow was successfully tested in the prolific Colombian hydrocarbon province of the Middle Magdalena Valley basin, and a 3D exploration scale facies model was constructed for the first time. The 3D model reproduces the structure of the basin (the major faults and the horizons bounding the oil producing Cenozoic fluvial formations of the La Paz, Esmeraldas, Mugrosa and Colorado) and the gross distribution of the reservoir and seal rocks.

3. The sedimentological analysis of the Middle Magdalena Valley basin distinguishes four facies associations: alluvial fan, overbank, floodplain and channel-fill deposits. The last one is the main reservoir rock and is composed of clean nonbioturbated very coarse to very fine-grained sandstones with subordinate conglomerates. In the well logs, this

facies exhibits a blocky-like expression with Vcl values equal to or below 40%, showing an upwards increasing trend and forming vertical sequences of more than 3 m (10 ft).

4. The seismic analysis shows that the major faults in the basin are NE – SW to N – S oriented and correspond to thrusts and faults with a reverse component in displacement. The tectonic activity ended earlier in the western margin of the basin, without affecting the deposition of the Colorado Fm. (i.e. before middle Miocene). In the eastern margin, the deformation was coeval with the sedimentation of this unit and with that of the Mugrosa Fm. (Oligocene–lower Miocene).

5. Within the modeling area, the La Paz Fm. is interpreted to exist in the northwestern margin. In general, the largest thicknesses of the Esmeraldas, Mugrosa and Colorado formations are distributed along the eastern margin and decrease towards the west. The southwest region corresponds to the depositional limit of the three units, where their bounding horizons onlap the U0 regional unconformity.

6. The fluvial style of the La Paz Formation in the subsurface of the MMVB is interpreted as mainly corresponding to a braided fluvial system, whereas meandering fluvial streams predominate in the Esmeraldas, Mugrosa and Colorado formations.

7. Paleogeographic reconstructions depict fluvial channel belts that describe combined transverse and longitudinal fluvial depositional systems, alluvial fans adjacent to the active basin margins and floodplain facies dominating the structural highs and the southwest depositional limit. The facies belt distribution is controlled by the structural evolution of the basin. The paleogeographic reconstructions were used to derive the lateral variograms used in the stochastic modeling.

8. The channel-fill facies association is shown in the 3D model as large geological bodies that interfinger with floodplain, overbank and alluvial fan deposits. The new areas of potential interest detected in the model are zones of high channel-fill facies probability

that form bodies that are isolated or terminate upwards in pinch-outs or truncations with faults. The 3D model of the MMVB may be regarded as a starting point for undertaking new studies and explorations in potentially interesting areas. Moreover, it could be used for developing subsequent models of petroleum systems.

9. The workflow developed and presented here can play a role in improving general exploration workflows in similar contexts.

REFERENCES

Aguiar, M. Y., and J. P. Reyes, 1982, Estudio estratigráfico del grupo Chorro en el sinclinal de Nuevo Mundo e interpretación del programa sísmico Nuevo Mundo-80, Bachelor's thesis, Universidad Nacional de Colombia, Bogotá, 67 p.

Allen, M. R., G. P. Goffey, R. K. Morgan, and I. M. Walker, 2006, The deliberate search for the stratigraphic trap: and introduction, *in* M. R. Allen, G. P. Goffey, R. K. Morgan, and I. M. Walker, eds., The deliberate search for the stratigraphic trap: Geological Society, London, Special Publications, v. 254, p. 1–5, doi: 10.1144/GSL.SP.2006.254.01.01.

Aspden, J. A., and W. J. McCourt, 1986, Mesozoic oceanic terrane in the central Andes of Colombia: Geology, v. 14, p. 415–418.

Aspden, J. A., W. J. McCourt, and M. Brook, 1987, Geometrical control of subduction-related magmatism: the Mesozoic and Cenozoic plutonic history of Western Colombia: Journal of the Geological Society, v. 144, p. 893–905.

Atkinson C. E., M. Renolds, and O. Hutapea, 2006, Stratigraphic traps in the Tertiary rift basins of Indonesia: case studies and future potential, *in* M. R. Allen, G. P. Goffey, R. K. Morgan, and I. M. Walker, eds., The deliberate search for the stratigraphic trap: Geological Society, London, Special Publications, v. 254, p. 105–126, doi: 10.1144/GSL.SP.2006.254.01.06.

Barrero, D., 1979, Geology of the central Western Cordillera, west of Buga and Roldanillo, Colombia: Ingeominas, Publicación Geológica Especial, v. 4, p. 1–75.

Barrero, D., A. Pardo, C. Vargas, and J. Martínez, 2007, Colombian sedimentary basins: Nomenclature, boundaries and petroleum geology, a new proposal: Bogotá, Agencia Nacional de Hidrocarburos, 91 p.

Biddle, K. T., and C. C. Wielchowsky, 1994, Hydrocarbon Traps, *in* L. B. Magoon, and W. G. Dow, eds., The petroleum system – from source to trap: AAPG Memoir 60, p. 219–235.

Biju-Duval, B., 2002, Sedimentary Geology. Sedimentary basins, depositional environments, petroleum formation: Paris, Éditions Technip and Institut Français du Pétrole, 642 p.

Caballero, V., 2010, Evolución tectono-sedimentaria del sinclinal del Nuevo Mundo, Cuenca sedimentaria Valle Medio del Magdalena Colombia, durante el Oligoceno-Mioceno, Master's thesis, Universidad Industrial de Santander, Bucaramanga, 157 p.

Caballero, V., et al., 2013, Tectonic controls on sedimentation in an intermontane hinterland basin adjacent to inversion structures: The Nuevo Mundo syncline, Middle Magdalena Valley, Colombia, *in* M. Nemčok, A. Mora, and J. W. Cosgrove, eds., Thick-skin-dominated orogens: from initial inversion to full accretion, Geological Society of London, Special Publications, v. 377, p. 315–342, doi: 10.1144/SP377.12.

Caballero, V., M. Parra, and A. Mora, 2010, Levantamiento de la Cordillera Oriental de Colombia durante el Eoceno tardío-Oligoceno temprano: Proveniencia sedimentaria en el sinclinal de Nuevo Mundo, cuenca Valle Medio del Magdalena: Boletín de Geología, v. 32, p. 45–77.

Caldwell, J., A. Chowdhury, P. van Bemmel, F. Engelmark, L. Sonneland, and N. S. Neidell, 1997, Exploring for stratigraphic traps: Oilfield Review, Winter 1997, p. 48–61.

Carll, J. F., 1880, The geology of the oil regions of Warren, Venango, Clarion, and Butler Counties, including surveys of the Garland and Panama conglomerates in Warren and Crawford, and in Chautauqua Co., N.Y., descriptions of oil well rig and tools, and a discussion of the preglacial and postglacial drainage of the Lake Erie country: Report of progress I.I.I.: Harrisburg, Second Pennsylvania Geological Survey, 482 p.

Carmona, A., O. Gratacós, R. C. Gispert, J. A. Muñoz, and S. Hardy, 2016, Numerical modelling of syntectonic subaqueous sedimentation: the effect of normal faulting and a relay ramp on sediment dispersal: Tectonophysics, v. 684, p. 100–118, doi: 10.1016/j.tecto.2016.06.018.

Catuneanu, O., 2006, Principles of sequence stratigraphy: Amsterdam, Elsevier, 375 p.

Cediel, F., R. P. Shaw, and C. Caceres, 2003, Assembly of the Northern Andean Block, *in* C. Bartolini, R. T. Buffer, and J. Blickwede, eds., The Circum-Gulf of Mexico and the Caribbean: Hydrocarbon habitats, basin formation, and plate tectonics: AAPG Memoir 79, p. 815–848.

Chew, D. M., U. Schaltegger, J. Kosler, M. J. Whitehouse, M. Gutjahr, R. A. Spikings and A. Miskovic, 2007, U-Pb geochronologic evidence for the evolution of the Gondwana margin of the north-central Andes: Geological Society of America Bulletin, v. 119, p. 697–711, doi: 10.1130/B26080.1.

Chopra, S., and K. Marfurt, 2005, Seismic attributes – A historical perspective: Geophysics, v. 50, 3SO-28SO, doi: 10.1190/1.2098670.

Cooper, M. A., et al., 1995, Basin development and tectonic history of the Llanos Basin, Eastern Cordillera and Middle Magdalena Valley, Colombia: AAPG Bulletin, v. 79, p. 1421–1443.

Cordani, U. G., K. Sato, W. Teixeira, C. C. G. Tassinari, and M. A. S. Basei, 2000, Crustal evolution of the South American platform, *in* U. G. Cordani, E. J. Miliani, A. Thomas-Filho, and D. A. Campos, eds., Tectonic evolution of South America: 31st International Geological Congress, Rio de Janeiro, Brazil, pp. 19–40.

Dengo, C. A., and M. C. Covey, 1993, Structure of the Eastern Cordillera of Colombia: Implications for trap styles and regional tectonics: AAPG Bulletin, v. 77, p. 1315–1337.

Deutsch, C. V., 2006, A sequential indicator simulation program for categorical variables with point and block data: BlockSIS: Computers and Geosciences, v. 32, p. 1669–1681, doi:10.1016/j.cageo.2006.03.005.

Deutsch, C. V., and A. G. Journel, 1998, GSLIB: Geostatistical Software Library and user's guide, 2nd ed.: Oxford, Oxford University Press, 350 pp.

Fabre, A., 1987, Tectonique et generation d’hydrocarbures: un modèle de evolution de la Cordillère Orientale de Colombie et du basin des Llanos pendant le Crétacé et le Tertiaire: Archive Science Genève, v. 40, p. 145–190.

Falivene, O., P. Cabello, P. Arbués, J. A. Muñoz, and L. Cabrera, 2009, A geostatistical algorithm to reproduce lateral gradual facies transitions: description and implementation: Computers and Geosciences, v. 35, p. 1642–1651, doi:10.1016/j.cageo.2008.12.003.

Falivene, O., A. Frascati, S. Gesbert, J. Pickens, Y. Hsu, and A. Rovira, 2014, Automatic calibration of stratigraphic forward models for predicting reservoir presence in exploration: AAPG Bulletin, v. 98, 1811–1935, doi: 10.1306/02271413028.

Gómez, E., T. E. Jordan, R. W. Allmendinger, K. Hegarty, S. Kelley, and M. Heizler, 2003, Controls on architecture of the Late Cretaceous to Cenozoic southern Middle Magdalena Valley Basin, Colombia: Geological Society of America Bulletin, v. 115, p. 131–147, doi:10.1130/0016-7606(2003)115<0131:COAOTL>2.0.CO;2.

Gómez, E., T. E. Jordan, R. W. Allmendinger, and N. Cardozo, 2005a, Development of the Colombian foreland-basin system as a consequence of diachronous exhumation of the northern Andes: Geological Society of America Bulletin, v. 117, p. 1272–1292, doi: 10.1130/B25456.1.

Gómez, E., T. E. Jordan, R. W. Allmendinger, K. Hegarty, and S. Kelley, 2005b, Syntectonic Cenozoic sedimentation in the northern middle Magdalena Valley Basin of Colombia and implications for exhumation of the Northern Andes: Geological Society of America Bulletin, v. 117, p. 547–569, doi: 10.1130/B25454.1.

Gómez, R. A., and J. Morales, 2008, Modelo geoestadístico basado en objetos de las formaciones Mugrosa y Colorado, Campo Lisama, Cuenca del Valle Medio del Magdalena, Colombia, Bachelor's thesis, Universidad Industrial de Santander, Bucaramanga, 157 p.

Gómez-Hernández, J. J., and R. M. Srivastava, 1990, ISIM3D: An ANSI-C three-dimensional multiple indicator conditional simulation program: Computers and Geosciences, v. 16, p. 395–440.

Gómez, J., et al., 2007, Mapa geológico de Colombia, Bogotá: INGEOMINAS, scale 1:1,000,000, 2 sheets.

Goovaerts, P., 2006, Geostatistical modeling of the spaces of local, spatial and response uncertainty for continuous petrophysical properties, *in* T. C. Coburn, J. M. Yarus, and R. L. Chambers, eds., Stochastic modelling and geostatistics: Principles, methods and case studies: AAPG Computer Applications in Geology 5, p. 59–79, doi:10.1306/1063807CA53229

Gordon, R., 1997, Stratigraphic Trap Classification, *in* C. E. Payton, ed., Seismic stratigraphy – Applications to hydrocarbon exploration: AAPG Memoir 26, p. 14–27.

Granjeon, D., 1996, Modélisation stratigraphique déterministe: Conception et applications d'un modèle diffusif 3D multilithologique, Ph.D. thesis, Université Rennes, Rennes, 189 p.

Granjeon, D., 2009, 3-D Stratigraphic modeling of sedimentary basins (abs.). AAPG Search and Discovery Article #90090, AAPG Annual Convention and Exhibition, Denver, Colorado, June 7–10, 2009.

Granjeon, D., 2010, Dionisos – 3D stratigraphic modelling of sedimentary basins: AAPG - ER Newsletter, v. 5, p. 4–5.

Granjeon, D., 2014, 3D forward modelling of the impact of sediment transport and base level cycles on continental margins and incised valleys, *in* A. W. Martinius, R. Ravnås, J. A. Howell, R. J. Steel, and J. P. Wonham, eds., From depositional systems to sedimentary successions on the Norwegian continental margin: Special

Publication of the International Association of Sedimentologists 46, p. 453 – 472, doi: 10.1002/9781118920435.ch16

Granjeon, D., and P. Joseph, 1999, Concepts and applications of a 3-D multiple lithology, diffusive model in stratigraphic modeling. Numerical experiments in stratigraphy: recent advances in stratigraphic and sedimentologic computer simulations. SEPM Special Publication 62, p. 197– 210.

Gratacós, O., K. Bitzer, J. L. Casamor, L. Cabrera, A. Calafat, M. Canals, and E. Roca, 2009, Simulating transport and deposition of clastic sediments in an elongate basin using the SIMSAFADIM-CLASTIC program: The Camarasa artificial lake case study (NE Spain): Sedimentary Geology, v. 222, p. 16–26, doi: 10.1016/j.sedgeo.2009.05.010

Hebrard, F., 1985, Les foothills de la Cordillère Orientale de Colombie entre les rios Casanare et Cusiana. Evolution géodynamique depuis l'Eo-Crétacé, Ph.D. thesis, Université Pierre et Marie Curie, Paris, 162 p.

Horton, B. K., 2012, Cenozoic evolution of hinterland basins in the Andes and Tibet, *in* C. Busby, and A. Azor, eds., Tectonics of sedimentary basins: Recent advances: Oxford, United Kingdom, Wiley-Blackwell, p. 427–444.

Horton, B. K., V. J. Anderson, V. Caballero, J. E. Saylor, J. Nie, M. Parra, and A. Maldonado, 2015, Application of detrital zircon U-Pb geochronology to surface and subsurface correlations of provenance, paleodrainage, and tectonics of the Middle Magdalena Valley Basin of Colombia: Geosphere, v. 11, p. 1790–1811, doi: 10.1130/GES01251.1

Horton, B. K., M. Parra, J. E. Saylor, J. Nie, A. Mora, V. Torres, D. F. Stockli, and M. R. Strecker, 2012, Resolving uplift of the northern Andes using detrital zircon age signatures: Geological Society of America Today, v. 20, p. 4–9, doi: 10.1130/GSATG76A.1.

Horton, B. K., J. E. Saylor, J. Nie, A. Mora, M. Parra, A. Reyes-Harker, and D. F. Stockli, 2010, Linking sedimentation in the northern Andes to the basement configuration, Mesozoic extension, and Cenozoic shortening: Evidence from detrital zircon U-Pb ages, Eastern Cordillera, Colombia: Geological Society of America Bulletin, v. 122, no. 9/10, p. 1423 – 1442, doi: 10.1130/B30118.1.

Jaillard, E., P. Solar, G. Carlier, and T. Mourier, 1990, Geodynamic evolution of the northern and central Andes during early to middle Mesozoic times: a Tethyan model: Journal of the Geological Society of London, v. 147, p. 1009–1022.

Journel, A. G., and F. Alabert, 1989, Non-Gaussian data expansion in the Earth Sciences: Terra Nova, v. 1, p. 123–134.

Koltermann, C. E., and S. M. Gorelick, 1996. Heterogeneity in sedimentary deposits: A review of structure-imitating, process-imitating, and descriptive approaches: Water Resources Research, v. 32, p. 2617–2658.

Levorsen, A. I., 1936, Stratigraphic versus structural accumulation: AAPG Bulletin, v. 20, p. 521–530.

Levorsen, A. I., 1967, Geology of Petroleum, 2nd ed.: San Francisco, W. H. Freeman and Co., 724 p.

Liu, J., K. Liu, and X. Huang, 2016, Effect of sedimentary heterogeneities on hydrocarbon accumulations in the Permian Shanxi Formation, Ordos Basin, China: Insight from an integrated stratigraphic forward and petroleum system modelling: Marine and Petroleum Geology, v. 76, 412–431, doi: 10.1016/j.marpetgeo.2016.05.028.

MacDonald, A. C., and J. O. Aasen, 1994, A prototype procedure for stochastic modeling of facies tract distribution in shoreface reservoirs, *in* J.M. Yarus, and R.L.

Chambers, eds., Stochastic modeling and geostatistics: Principles, methods, and case studies: AAPG Computers Applications in Geology 3, p. 91–108.

McCourt, W. J., J. A. Aspden, and M. Brook, 1984, New geological and geochronological data from the Colombian Andes: continental growth by multiple accretion: Journal of the Geological Society, v. 141, p. 831–845.

Mora, A., B. K. Horton, A. Mesa, J. Rubiano, R. A. Ketcham, M. Parra, V. Blanco, D. Garcia, and D. F. Stockli, 2010, Migration of Cenozoic deformation in the Eastern Cordillera of Colombia interpreted from fission track results and structural relationships: Implications for petroleum systems: AAPG Bulletin, v. 94, p. 1543–1580, doi: 10.1306/01051009111.

Mora, A., M. Parra, M. R. Strecker, A. Kammer, C. Dimaté, and F. Rodríguez, 2006, Cenozoic contractional reactivation of Mesozoic extensional structures in the Eastern Cordillera of Colombia: Tectonics, v. 25, doi: 10.1029/2005TC001854 2010.

Morales, L. G., et al., 1958, General geology and oil occurrences of Middle Magdalena Valley, Colombia: South America, *in* L. G. Weeks, ed., SP 18: Habitat of Oil: AAPG Special Volumes, p. 641–695.

Moreno, C. J., B. K. Horton, V. Caballero, A. Mora, M. Parra, and J. Sierra, 2011, Depositional and provenance record of the Paleogene transition from foreland to hinterland basin evolution during Andean orogenesis, northern Middle Magdalena Valley Basin, Colombia: Journal of South American Earth Sciences, v. 32, p. 246–263, doi: 10.1016/j.jsames.2011.03.018.

Nie, J., B. H. Horton, A. Mora, J. E. Saylor, T. B. Housh, J. Rubiano, and J. Naranjo, 2010, Tracking exhumation of Andean ranges bounding the Middle Magdalena Valley Basin, Colombia: Geology, v. 38, p. 451–454, doi: 10.1130/G30775.1.

Neumaier, M., R. Littke, T. Hantschel, L. Maerten, J-P. Joonnekindt, and P. Kukla, 2014, Integrated charge and seal assessment in the Monagas fold and thrust belt of Venezuela: AAPG Bulletin, v. 98, no. 7, p. 1325–1350, doi: 10.1306/01131412157.

Parra, M., A. Mora, C. Jaramillo, M. R. Strecker, E. R. Sobel, L. Quiroz, M. Rueda, and V. Torres, 2009, Orogenic wedge advance in the northern Andes: Evidence from the Oligocene-Miocene sedimentary record of the Medina Basin, Eastern Cordillera, Colombia, Geological Society of America Bulletin, v. 121, p. 780–800, doi: 10.1130/B26257.1.

Parra, M., A. Mora, C. Lopez, L. E. Rojas, and B. K. Horton, 2012, Detecting earliest shortening and deformation advance in thrust-belt hinterlands: Example from the Colombian Andes: Geology, v. 40, p. 175–178, doi: 10.1130/G32519.1.

Ramon, J. C., L. Dzou, and B. Giraldo, 1997, Geochemical evaluation of the Middle Magdalena basin, Colombia, Ciencia, Tecnología y Futuro, v. 1, p. 47–66.

Restrepo-Pace, P. A., F. Colmenares, C. Higuera, and M. Mayorga, 2004, A fold and-thrust belt along the western flank of the Eastern Cordillera of Colombia-Style, kinematics, and timing constraints derived from seismic data and detailed surface mapping, *in* K.R. McClay, ed., Thrust tectonics and hydrocarbon systems: AAPG Memoir 82, p. 598–613.

Reyes-Harker, A., et al., 2015, Cenozoic paleogeography of the Andean foreland and retroarc hinterland of Colombia: AAPG Bulletin, v. 99, p. 1407–1453, doi:10.1306/06181411110.

Rittenhouse, G., 1972, Stratigraphic trap classification, *in* R. E. King, ed., Stratigraphic oil and gas fields – classification, exploration methods, and case histories: AAPG Memoir 16, p. 14–28.

Rolon, L. F., 2004, Structural geometry of the Jura-Cretaceous rift of the Middle Magdalena Valley Basin, Colombia. Master's thesis, West Virginia University, Morgantown, 63 p.

Sánchez, J., B. K. Horton, E. Tesón, A. Mora, R. A. Ketcham, and D. F. Stockli, 2012, Kinematic evolution of Andean fold-thrust structures along the boundary between the Eastern Cordillera and Middle Magdalena Valley basin, Colombia: Tectonics, v. 31, TC3008, doi:10.1029/2011TC003089.

Sánchez, N., A. Mora, M. Parra, D. Garcia, M. Cortes, T. M. Shanahan, R. Ramirez, O. Llamosa, and M. Guzman, 2015, Petroleum system modeling in the Eastern Cordillera of Colombia using geochemistry and timing of thrusting and deformation: AAPG Bulletin, v. 99, p. 1537–1556, doi: 10.1306/04161511107.

Sarmiento, L. F., 2001, Mesozoic rifting and Cenozoic basin inversion history of the Eastern Cordillera, Colombian Andes. Inferences from tectonic models, Ph.D. thesis, Vrije University, Amsterdam, 295 p.

Sarmiento, L. F., 2011, Petroleum geology of Colombia, Middle Magdalena Basin: Medellin, Agencia Nacional de Hidrocarburos, 193 p.

Saylor, J. E., B. K. Horton, J. Nie, J. Corredor, and A. Mora, 2011, Evaluating foreland basin partitioning in the northern Andes using Cenozoic fill of the Floresta basin, Eastern Cordillera, Colombia: Basin Research, v. 23, p. 377–402, doi:10.1111/j.1365-2117.2010.00493.x.

Schamel, S., 1991, Middle and Upper Magdalena Basins, Colombia, *in* K.T. Biddle, ed., Active margin basins: AAPG Memoir 52, p. 283–301.

Seyfang, B., T. Aigner, D. K. Munsterman, and A. Irmen, 2017, An integrated workflow to assess the remaining potential of mature hydrocarbon basins: a case study from Northwest Germany (Upper Jurassic/Lower Cretaceous, Lower Saxony Basin): International Journal of Earth Sciences, v. 106, 1075–1105, doi: 10.1007/s00531-016-1354-8.

Slatt, R. M., 2006, Stratigraphic reservoir characterization for petroleum geologists, geophysicists and engineers: Amsterdam, Elsevier, 478 p.

Spickert, A., 2014, Petroleum system analysis: Middle Magdalena Valley Basin, Colombia, South America, Master's thesis, University of Washington, 48 pp.

Spikings, R., R. Cochrane, D. Villagomez, R. Van der Lelij, C. Vallejo, W. Winkler, and B. Beate, 2015, The geological history of northwestern South America: From Pangaea to the early collision of the Caribbean large igneous province (290-75Ma): Gondwana Research, v. 27, no. 1, p. 95–139.

Strohmenger, C. J., et al., 2006, Sequence stratigraphy and reservoir architecture of the Burgan and Mauddud formations (Lower Cretaceous), Kuwait, *in* P. M. Harris and L. J. Weber, eds., Giant hydrocarbon reservoirs of the world: From rocks to reservoir characterization and modeling: AAPG Memoir 88/SEPM Special Publication, p. 213–245.

Suárez, M. A., 1996, Facies analysis of the Upper Eocene La Paz Formation, and regional evaluation of the Post-Middle Eocene stratigraphy, Northern Middle Magdalena Valley Basin, Colombia, Master's thesis, University of Colorado, Boulder, 104 p.

Torrado, L., P. Mann, and J. Bhattacharya, 2014, Application of seismic attributes and spectral decomposition for reservoir characterization of a complex fluvial system: Case study of the Carbonera Formation, Llanos foreland basin, Colombia: Geophysics, v. 79, p. B221–230, 10.1190/GEO2013-0429.1

Tyler, N., and R. J. Finley, 1991, Architectural controls on the recovery of hydrocarbons from sandstone reservoirs, *in* A. D. Miall, and N. Tyler, eds., The three-dimensional facies architecture of terrigenous clastic sediments and its implications for

hydrocarbon discovery and recovery. Concepts in sedimentology and paleontology: Society for Sedimentary Geology, p. 1–5.
Van der Hammen, T., 1961, Late Cretaceous and Tertiary stratigraphy and tectonogenesis of the Colombian Andes: Geologie en Mijnbouw, v. 40, p. 181–188.
Veeken, P. C. H., 2007, Seismic stratigraphy, basin analysis and reservoir characterization. Handbook of geophysical exploration, seismic exploration: Amsterdam, Elsevier, 509 p.
Veiga, R., and F. Dzelalija, 2014, A Regional overview of the La Luna Formation and the Villeta Group as shale gas/shale oil in the Catatumbo, Magdalena Valley and Eastern Cordillera Regions, Colombia, AAPG Search and Discovery Article #10565, 21 p.
Villagómez, D., and D. Spikings, 2013, Thermochronology and tectonics of the Central and Western Cordilleras of Colombia: Early Cretaceous-Tertiary evolution of the Northern Andes: Lithos, v. 160-161, p. 228–249.

AUTHORS

Patricia Cabello ~ Department de Dinàmica de la Terra i de l'Oceà, Universitat de Barcelona, Facultat de Ciències de la Terra, c/ Martí i Franquès s/n, 08028 Barcelona, Spain; pcabello@ub.edu

Patricia is lecturer at the University of Barcelona and is a member of the Geomodels Research Institute and the Research Group of Geodynamics and Basin Analysis. She received her Ph.D. from the University of Barcelona in 2010. Her research is mainly focused on the characterization of reservoirs and outcrop analogs.

Cristina Lopez Arias ~ Ecopetrol S. A, Bogotá, Colombia; cristina.lopez@ecopetrol.com.co

Cristina is senior exploration geologist at Ecopetrol S.A. She received her B.Sc. in geology from the National University of Colombia and her M.Sc. from the University of Barcelona and the Autonomous University of Barcelona. She has worked on regional exploration and prospection projects in Colombia. Her research interests include sedimentology, reservoir prediction and structural geology.

Néstor Gamba Ruiz ~ Ecopetrol S. A., Bogotá, Colombia; nestor.gamba@ecopetrol.com.co

Néstor Gamba is senior geologist at Ecopetrol S. A. He has a B.Sc. in geology from the Universidad Nacional de Colombia and a M.Sc. from the University of Barcelona and the Autonomous University of Barcelona. He is currently working on regional exploration projects of several basins in Colombia. His research interests include stratigraphy and sedimentology.

Maria Isabel Dussán Lubert ~ Ecopetrol, Bogotá, Colombia; maria.dussan@ecopetrol.com.co

Maria Isabel Dussán is senior exploration geologist in Ecopetrol S. A. She has a B.Sc. from the Universidad de Caldas and M. Sc. from the University of Barcelona and the Autonomous University of Barcelona. Her research is focused on the generation of exploratory opportunities in Colombian basins. She is currently working on exploration projects in the Eastern Cordillera in Colombia.

Elena Torres Torres ~ Ecopetrol S. A., Bogotá, Colombia; Elena.Torres@ecopetrol.com.co

Elena Torres is a geologist at Ecopetrol S.A. Her areas of expertise are petrography, petrophysics, sedimentology and stratigraphy. She has worked in various basins in Colombia (Middle Magdalena Valley, Llanos Foreland and Foothills, Catatumbo) and has wide experience in regional studies. She received her B.Sc. degree from the Universidad Nacional de Colombia.

César Iván Ballesteros Torres ~ Ecopetrol S. A., Bogotá D. C., Colombia; cesar.ballesteros@ecopetrol.com.co

César Iván Ballesteros Torres received his B.Sc. in geology from the Universidad Nacional de Colombia, Bogotá, and his M.Sc. from the University of South Carolina, Columbia, USA. He joined Ecopetrol in 1998 and has worked as a seismic interpreter in the Middle Magdalena Valley Basin, looking for and evaluating new exploration opportunities in the Cretaceous and Tertiary sequences.

Maria Teresa Cantisano ~ Ecopetrol S. A., Bogotá D. C., Colombia; Maria.Cantisano@ecopetrol.com.co

Maria Teresa is senior engineering geologist at Ecopetrol S. A. She received her M. Sc. from the Universidad Central de Venezuela. She has wide experience in the geological and petrophysical characterization of clastic and carbonate rocks in the Exploration and Production areas. She has worked in hydrocarbon basins of Venezuela, Trinidad and Tobago, Argentina and Colombia.

Nelbett Marfisi ~ Ecopetrol S. A., Bogotá, Colombia; Nelbett.marfisi@ecopetrol.com.co

Nelbett is senior sedimentologist at Ecopetrol S. A. and is a member of the multidisciplinary team of unconventional resources. She works to maintain the national oil industry at the forefront of new technologies. She received her B.Sc. in engineering geology from the Universidad de Oriente and M.Sc. in earth sciences from the Universidad Central de Venezuela.

Rubén Calvo ~ Departament de Geologia, Facultat de Ciències, Universitat Autònoma de Barcelona, 08193 Bellaterra, Spain; Ruben.Calvo@uab.cat

Rubén Calvo is lecturer in geology at the Autonomous University of Barcelona. He received his B.Sc. (2008) and M.Sc. (2009) from the University of Barcelona, and was awarded his Ph. D. in 2016. His main areas of expertise include fluvial sedimentology and stratigraphy, and his research is focused on the multidisciplinary and integrated study of sedimentary basins.

Yaniel Misael Vázquez Taset ~ Escuela de Ciencias Geológicas e Ingeniería, Universidad Experimental Yachay Tech, Urcuquí, Ecuador; yvazquez@yachaytech.edu.ec

Yaniel Vázquez is lecturer and researcher in stratigraphy and basin analysis at Yachay Tech University. He received his B. Sc. in geology from the Instituto Superior Minero Metalúrgico de Moa "Antonio Núñez Jiménez", Cuba, and his Ph.D. from the University of Barcelona in 2014. His research interests include basin analysis, structural and petroleum geology.

Emilio Ramos ~ Department de Dinàmica de la Terra i de l'Oceà, Universitat de Barcelona, Facultat de Ciències de la Terra, c/ Martí i Franquès s/n, 08028 Barcelona, Spain; emilio.ramos@ub.edu

Emilio was awarded his Ph.D. in geology at the University of Barcelona in 1988. Since then, he has held a post as lecturer in basin analysis and petroleum geology at the same university. He has worked on several research projects on sedimentology and basin analysis in Spain, North Africa, Antarctica and South America.

FIGURE CAPTIONS

Figure 1. Geological map showing the main sedimentary basins and ranges in the northern Andean Range in Colombia. The red inbox indicates the study area in the Middle Magdalena Valley basin. Modified from Gómez et al. (2007). See the geological sketch in the lower right inset, in which the area of the geological map is indicated. MVB refers to the Magdalena Valley Basin.

Figure 2. Tectono-stratigraphic (**a**) and chrono-stratigraphic (**b**) subdivision of the Middle Magdalena Valley basin sedimentary infill. MMVU stands for Middle Magdalena Valley Unconformity. Modified from Suárez (1996) and Gómez et al. (2005b).

Figure 3. Workflow used in this study for defining new areas of potential interest in the Middle Magdalena Valley basin. TTG stands for the algorithm based on the truncation of the sum of a deterministic linear expectation trend and a Gaussian random field, which

was used to model the transition from alluvial fan to fluvial deposits. SIS stands for Sequential Indicator Simulation, used to model the fluvial facies associations.

Figure 4. Location of the wells and seismic lines used in this study. A geological sketch of the location of the outcrops under study is shown in the eastern half of the area. The position of the seismic profiles in Figure 9, the cross-sections in Figure 14 and the diagram in Figure 15 are indicated. Coordinates are shown in both the Geographic coordinate system and the Universal Transverse Mercator (UTM) (Colombia Bogota Zone).

Figure 5. Field views (a, c, f and g) and images from cores (b, d and e) showing some examples of the facies associations distinguished in the outcrops and in the subsurface. Alluvial fan deposits (facies association A): **a)** Close-up of massive, poorly-sorted silty sandstone (lithofacies SMm; see Table 2 and Figure 6a) with floating clasts (red arrows) resulting from the deposition of unconfined mudflows in the middle part of an alluvial fan. Mugrosa Fm. in outcrop 5. **b)** Poorly-sorted, matrix-supported breccia interpreted as proximal alluvial fan deposits. Channel-fill deposits (facies association C): **c)** General view of the stacking of the fluvial channel-fill sequences displaying lateral accretion surfaces (red arrows). Esmeraldas Fm. in outcrop 4. **d)** Rounded to well rounded, clast-supported conglomerates with erosional bottom surface (white dashed line). **e)** Large-scale cross-laminated sandstone. Overbank deposits (facies association O): **f)** 1 – 2 m (3.3 – 6.6 ft) thick, overbank sequences in the middle part of the La Paz Fm. in outcrop 2. The lower sequence is capped by a distributary overflow channel with an erosive basal surface (red arrow). See also Figure 6f. Floodplain deposits (facies association F): **g)** Thick interval of floodplain deposits in the lower part of the Colorado Fm. in outcrop 7. The massive red mudstones contain scattered carbonate nodules (lithofacies Mmn; Table 2

and Figure 6i), which locally form discontinuous horizons (red arrows). See outcrop locations in Figure 4.

Figure 6. Facies associations and sequences: **a-c**) Distal to middle alluvial fan (A) facies association. **d-e**) Channel-fill (C) sequences; **f**) Overflow (O) sequence; **g-j**) Floodplain (F) facies association. See text and Table 2 for more details. Proposed facies models: **(k)** fluvial-alluvial fan system; **(l)** straight braided channel; and **(m)** high sinuosity meandering channel.

Figure 7. Schematic logs of the outcrops showing the facies associations, paleocurrent trends and facies association proportions. Vertical separation between logs is not to scale. Paleocurrent data include our own measures, and data from Aguiar and Reyes (1982), Gómez et al. (2005a) and Caballero et al. (2009). Facies association percentages for outcrop 1 refer only to the La Paz Formation.

Figure 8. a) Map of the study area showing the major faults in the Middle Magdalena Valley basin, which were included in the 3D geological model. The traces correspond to the intersection between the unconformity U0 and the fault surfaces. Names correspond to widespread fault names used in the area. Coordinates are indicated in both the Geographic coordinate system and the Universal Transverse Mercator (UTM) (Colombia Bogota Zone). **b)** Chronology of the fault activity during the deposition of the stratigraphic units inferred from the seismic interpretation. See two seismic profiles and the corresponding interpretation in Figure 9.

Figure 9. a) Seismic profile and corresponding interpretation showing the relationship between Cantagallo and Cantagallo Este faults and the stratigraphic units in the Middle Magdalena Valley basin. **b)** Seismic profile and corresponding interpretation showing the relationship between the Provincia fault and its back thrust and the stratigraphic units in the Middle Magdalena Valley basin. See location of both profiles in Figure 4.

Figure 10. Three-dimensional model of the Middle Magdalena Valley basin showing the stratigraphic and structural framework (a to f) and the geostatistical facies distribution (g and h). **a)** Tertiary basal unconformity (U0) and major faults. See the trace of the intersection between the faults and U0, and the names of the faults in figure 8. **b)** U0 and top of the La Paz Formation. **c)** Top of the Esmeraldas Formation (U1) onlapping the basal unconformity U0 in the SW corner of the study area. **d)** Top of the Mugrosa Formation (U2) onlapping the U0 also in the SW. **e)** Top of the Colorado Formation (U3), also onlapping pre-existing surfaces to the SW. **f)** Modeling zones corresponding to each stratigraphic unit. **g)** One realization of the 3D geocellular facies model reproducing the distribution of the facies associations. **b)** 3D parameter showing the probability of occurrence of channel-fill sandstone bodies resulting from averaging the twenty realizations of the 3D facies model. Coordinates are in the Universal Transverse Mercator (UTM) system, Colombia Bogota Zone. Vertical scale is indicated in feet and exaggeration is 4x.

Figure 11. True vertical thickness maps of the four stratigraphic units extracted from the 3D model. **a)** La Paz Fm. (Lower tectonosequence 1, TS1) **b)** Esmeraldas Fm. (Upper TS1). **c)** Mugrosa Fm. (tectonosequence 2, TS2). **d)** Colorado Fm. (tectonosequence 3, TS3). Coordinates are indicated in both the Geographic coordinate system and the Universal Transverse Mercator (UTM) (Colombia Bogota Zone).

Figure 12. Proportion maps of the channel-fill facies associations for the four stratigraphic units studied. **a)** La Paz Fm. (Lower tectonosequence 1, TS1) **b)** Esmeraldas Fm. (Upper TS1). **c)** Mugrosa Fm. (tectonosequence 2, TS2). **d)** Colorado Fm. (tectonosequence 3, TS3). Coordinates are shown in both the Geographic coordinate system and the Universal Transverse Mercator (UTM) (Colombia Bogota Zone).

Figure 13. Cross-sections of the 3D facies model of the Middle Magdalena Valley basin and the 3D channel-fill sandstone probability parameter derived from the 3D facies model in longitudinal **(a)** and transversal **(b)** directions. See the position of the cross-sections in Figure 4.

Figure 14. Paleogeographic reconstruction of the four stratigraphic units. **a)** La Paz Formation (lower tectonosequence 1, TS1); **b)** Esmeraldas Formation (Upper TS1); **c)** Mugrosa Fm. (tectonosequence 2, TS2); **d)** Colorado Fm. (tectonosequence 3, TS3). Coordinates are indicated in both the Geographic coordinate system and the Universal Transverse Mercator (UTM) (Colombia Bogota Zone).

Figure 15. Portions of the 3D parameter representing the probability of channel-fill sandstone facies in the 3D facies model and corresponding cross-sections, showing areas of interest associated with potential hydrocarbon traps. Vertical exaggeration of the 3D parameters is 4x.

Figure 16. Diagram of the 3D parameter representing the channel-fill probability in the 3D facies model of the Middle Magdalena Valley basin and the facies association well log for the wells used to calibrate the model. The percentages represent the degree of agreement between the corresponding well and the 3D probability parameter. See the location of the calibration wells and the diagram in Figure 4.

Table 1. Variogram data and global facies proportions used in the 3D facies modeling of the Middle Magdalena Valley basin. *Rhmax* indicates the variogram range in the direction of maximum correlation in a horizontal plane, which corresponds to the azimuth direction. *Rhmin* refers to the variogram range in the direction of minimum correlation in a horizontal plane. *Rv* indicates the variogram range in the vertical direction. The facies proportions represent the average values from the upscaled facies association well logs.

Table 2. Summarized description and interpretation of the eighteen lithofacies from the outcrops under study in the Middle Magdalena Valley basin.

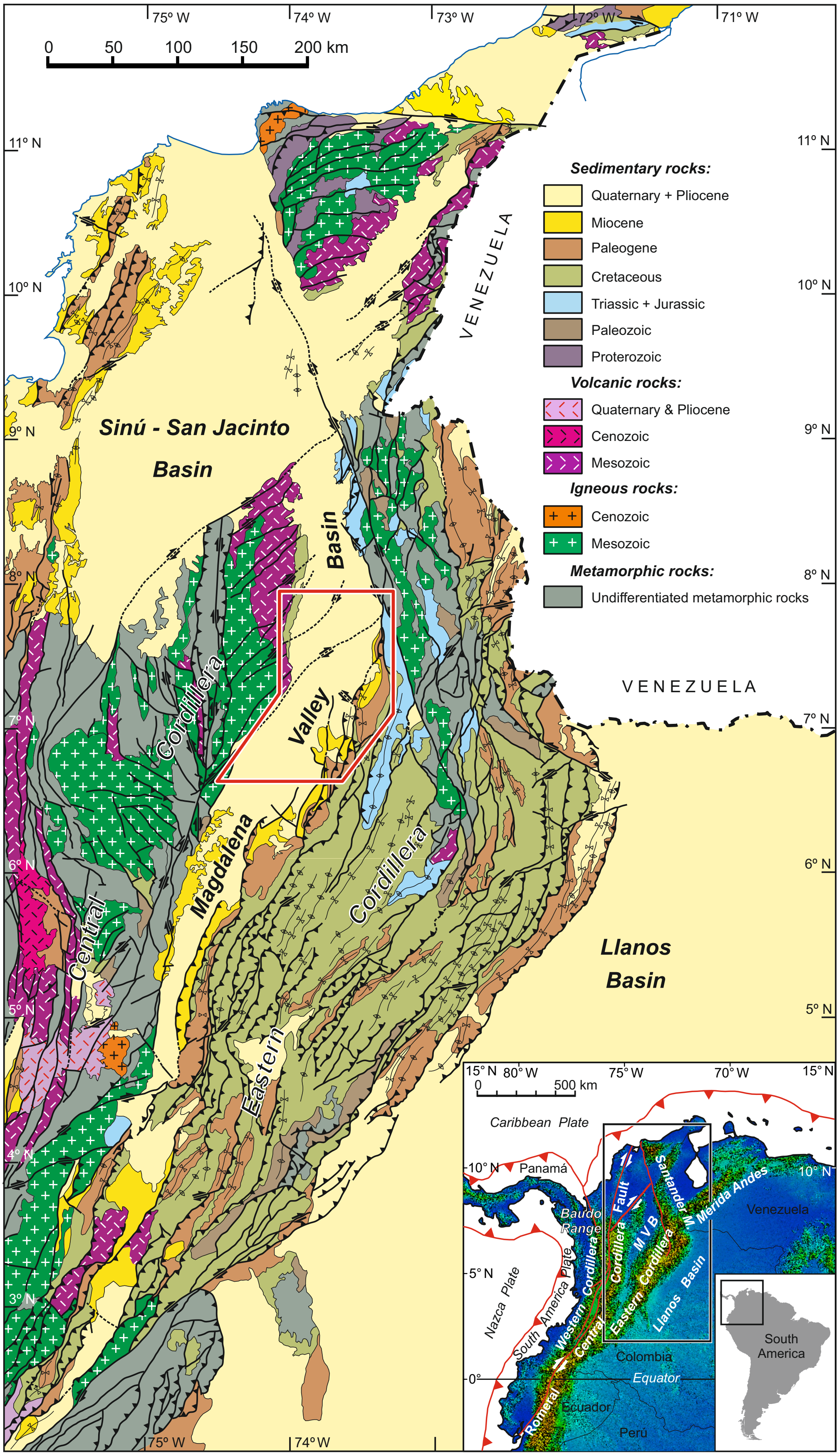

75° W
74° W
73° W
72° W
71° W
0 50 100 150 200 km
11° N
10° N
9° N
8° N
7° N
6° N
5° N
4° N
3° N
Sedimentary rocks:
Quaternary + Pliocene
Miocene
Paleogene
Cretaceous
Triassic + Jurassic
Paleozoic
Proterozoic
Volcanic rocks:
Quaternary & Pliocene
Cenozoic
Mesozoic
Igneous rocks:
Cenozoic
Mesozoic
Metamorphic rocks:
Undifferentiated metamorphic rocks
VENEZUELA
Sinú - San Jacinto
Basin
Basin
Valley
Cordillera
Magdalena
Central
Cordillera
Eastern
Llanos
Basin
15° N
80° W
75° W
70° W
0 500 km
Caribbean Plate
10° N
Panamá
Baudo
Range
Fault
Santander
M V B
Merida Andes
Venezuela
5° N
Nazca Plate
South America Plate
Western Cordillera
Cordillera
Central
Eastern
Cordillera
Llanos Basin
Colombia
Equator
0°
Romeral
Ecuador
Perú
South
America

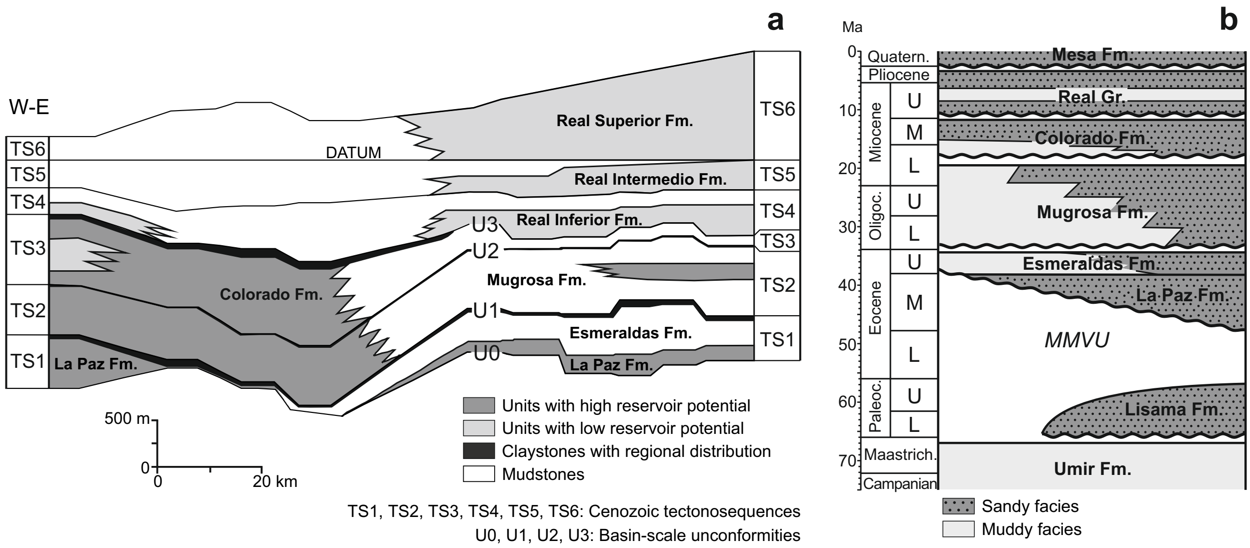

a
W-E
TS6
TS5
TS4
TS3
TS2
TS1
DATUM
Real Superior Fm.
Real Intermedio Fm.
Real Inferior Fm.
U3
U2
U1
U0
Colorado Fm.
Mugrosa Fm.
Esmeraldas Fm.
La Paz Fm.
500 m
0
0
20 km
Units with high reservoir potential
Units with low reservoir potential
Claystones with regional distribution
Mudstones
TS1, TS2, TS3, TS4, TS5, TS6: Cenozoic tectonosequences
U0, U1, U2, U3: Basin-scale unconformities
b
Ma
0
10
20
30
40
50
60
70
Quatern.
Pliocene
Miocene
Oligoc.
Eocene
Paleoc.
Maastrich.
Campanian
U
M
L
Mesa Fm.
Real Gr.
Colorado Fm.
Mugrosa Fm.
Esmeraldas Fm.
La Paz Fm.
MMVU
Lisama Fm.
Umir Fm.
Sandy facies
Muddy facies

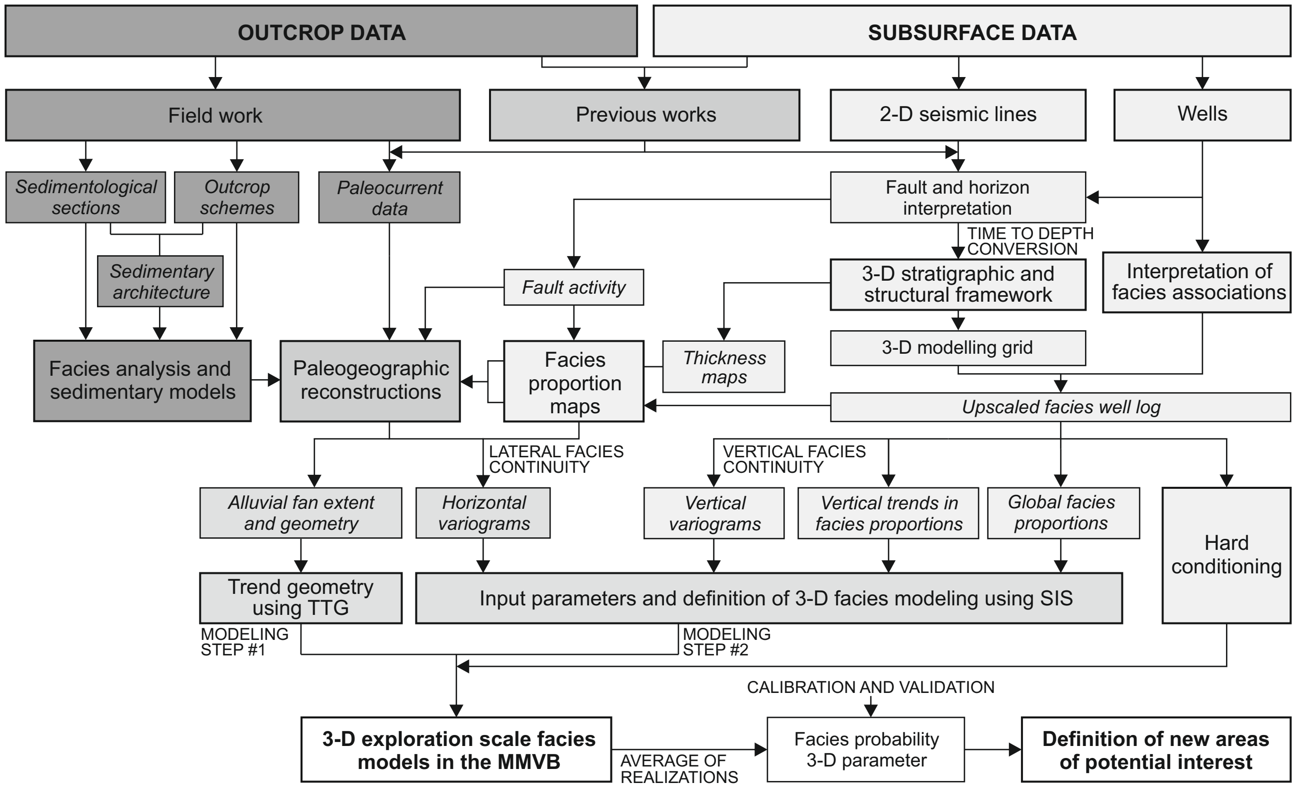
OUTCROP DATA
SUBSURFACE DATA
Field work
Previous works
2-D seismic lines
Wells
Sedimentological sections
Outcrop schemes
Paleocurrent data
Fault and horizon interpretation
TIME TO DEPTH CONVERSION
Sedimentary architecture
Fault activity
3-D stratigraphic and structural framework
Interpretation of facies associations
Facies analysis and sedimentary models
Paleogeographic reconstructions
Facies proportion maps
Thickness maps
3-D modelling grid
Upscaled facies well log
LATERAL FACIES CONTINUITY
VERTICAL FACIES CONTINUITY
Alluvial fan extent and geometry
Horizontal variograms
Vertical variograms
Vertical trends in facies proportions
Global facies proportions
Hard conditioning
Trend geometry using TTG
Input parameters and definition of 3-D facies modeling using SIS
MODELING STEP #1
MODELING STEP #2
CALIBRATION AND VALIDATION
3-D exploration scale facies models in the MMVB
AVERAGE OF REALIZATIONS
Facies probability 3-D parameter
Definition of new areas of potential interest

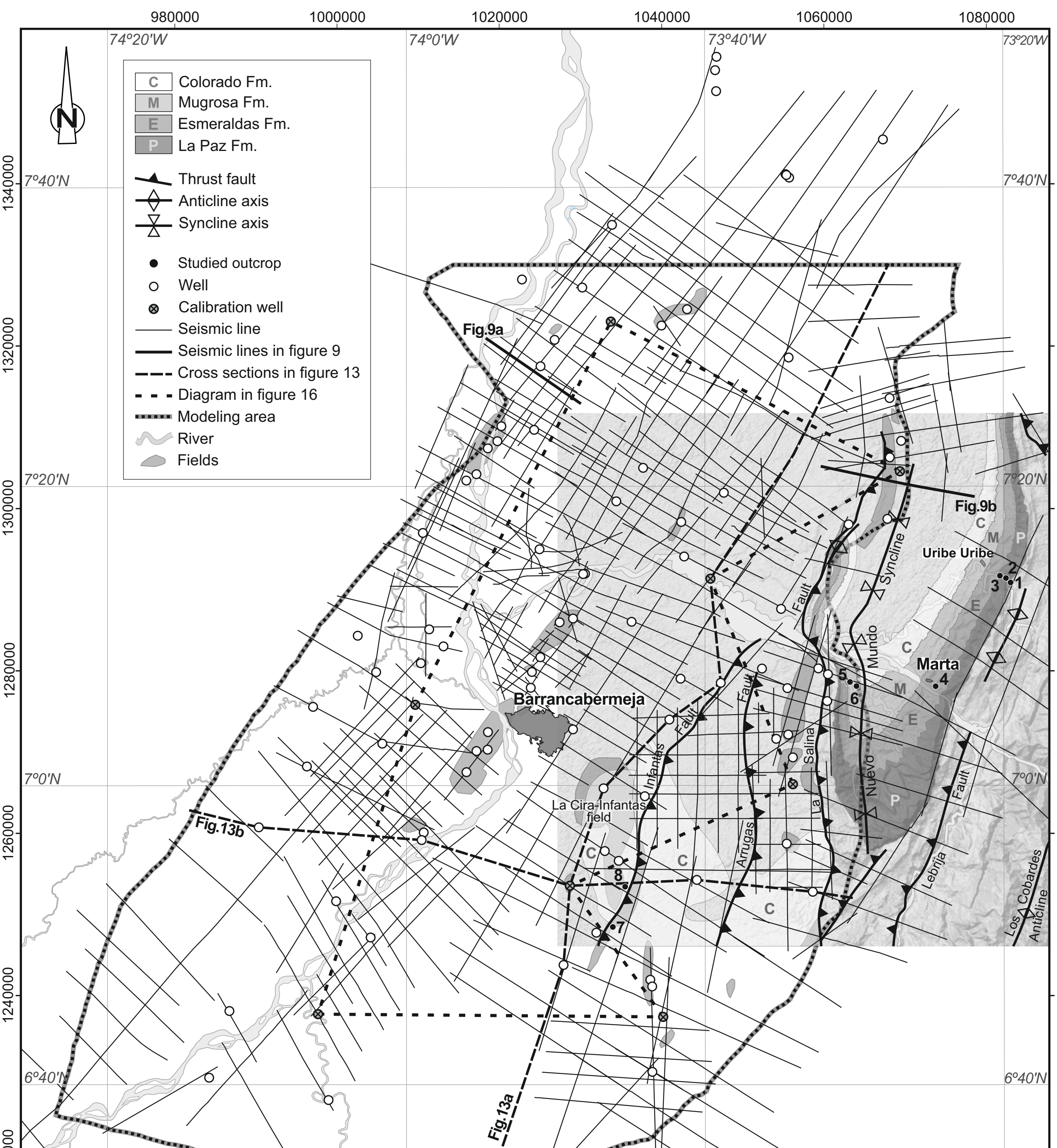

C Colorado Fm.
M Mugrosa Fm.
E Esmeraldas Fm.
P La Paz Fm.
Thrust fault
Anticline axis
Syncline axis
Studied outcrop
Well
Calibration well
Seismic line
Seismic lines in figure 9
Cross sections in figure 13
Diagram in figure 16
Modeling area
River
Fields
N
980000
1000000
1020000
1040000
1060000
1080000
1340000
1320000
1300000
1280000
1260000
1240000
1220000
74°20'W
74°0'W
73°40'W
73°20'W
7°40'N
7°20'N
7°0'N
6°40'N
Fig.9a
Fig.9b
Fig.13a
Fig.13b
Barrancabermeja
La Cira-Infantas field
Infantas Fault
Arrugas Fault
La Salina Fault
Nuevo Mundo Syncline
Lebrija Fault
Los Cobardes Anticline
Uribe Uribe
Marta
0 10 20 km

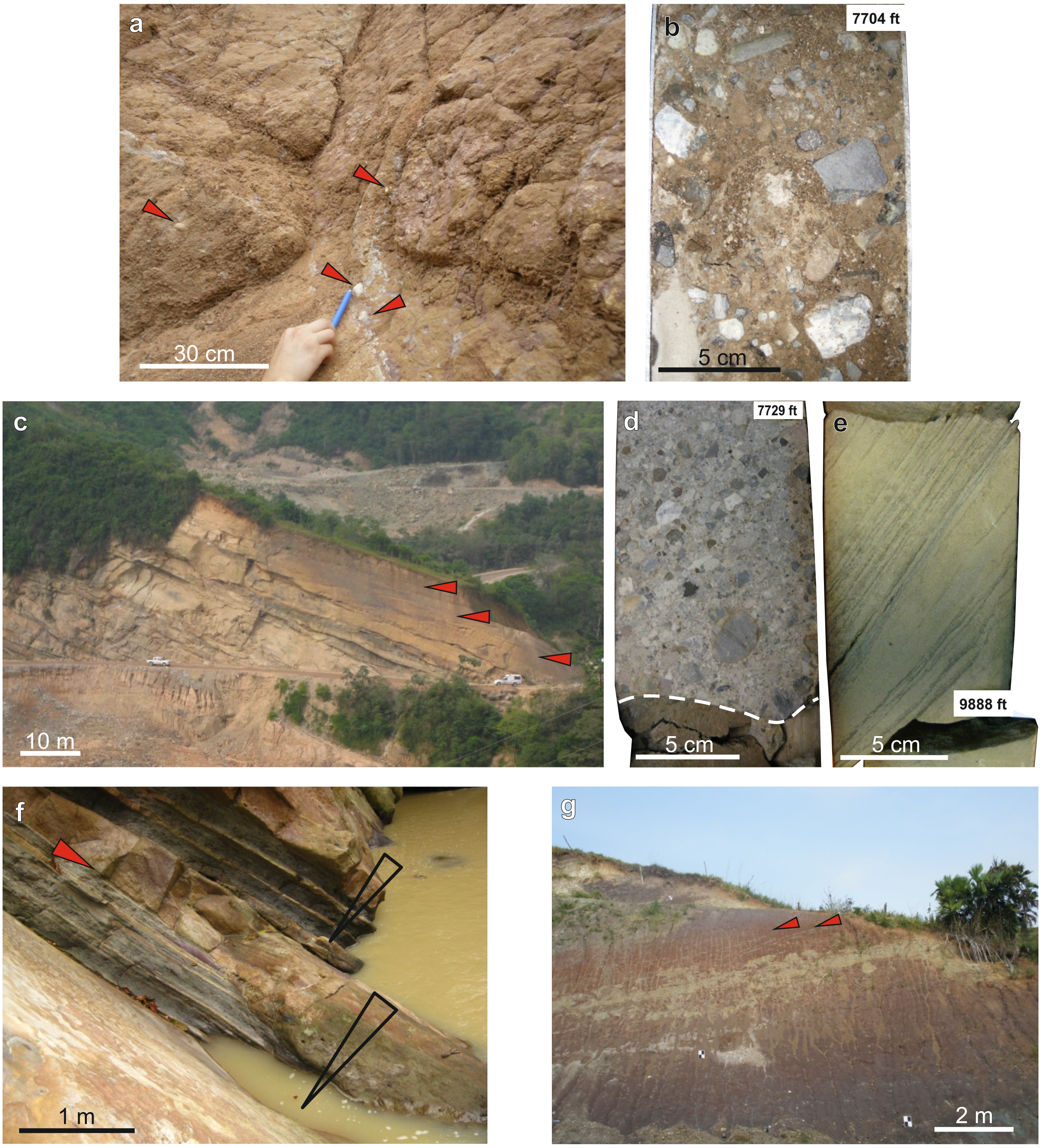
a
30 cm
b
7704 ft
5 cm
c
10 m
d
7729 ft
5 cm
e
9888 ft
5 cm
f
1 m
g
2 m

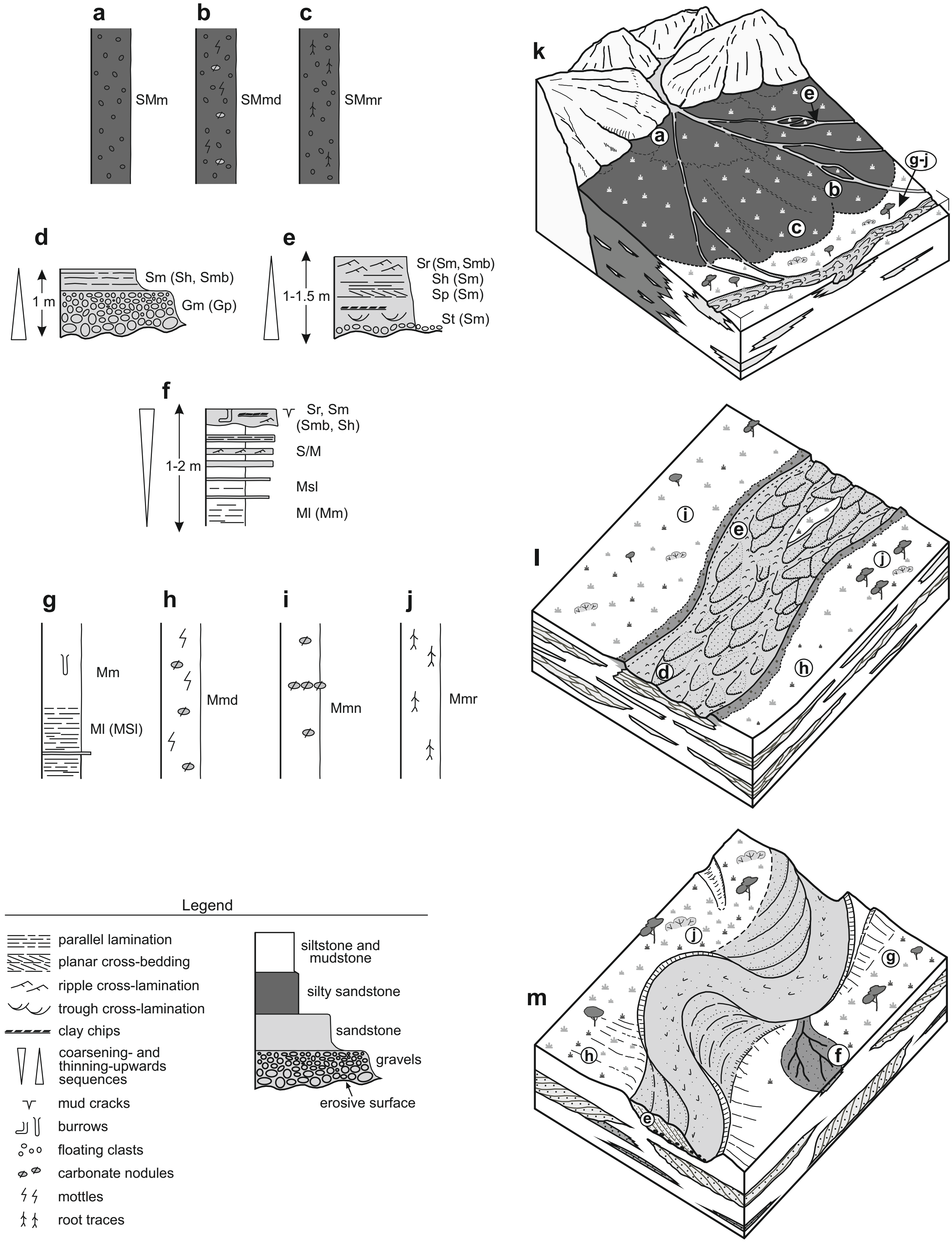

a
b
c
SMm
SMmd
SMmr
d
1 m
Sm (Sh, Smb)
Gm (Gp)
e
1-1.5 m
Sr (Sm, Smb)
Sh (Sm)
Sp (Sm)
St (Sm)
f
1-2 m
Sr, Sm
(Smb, Sh)
S/M
Msl
Ml (Mm)
g
h
i
j
Mm
Ml (MSl)
Mmd
Mmn
Mmr
k
l
m
g-j
Legend
parallel lamination
planar cross-bedding
ripple cross-lamination
trough cross-lamination
clay chips
coarsening- and thinning-upwards sequences
mud cracks
burrows
floating clasts
carbonate nodules
mottles
root traces
siltstone and mudstone
silty sandstone
sandstone
gravels
erosive surface

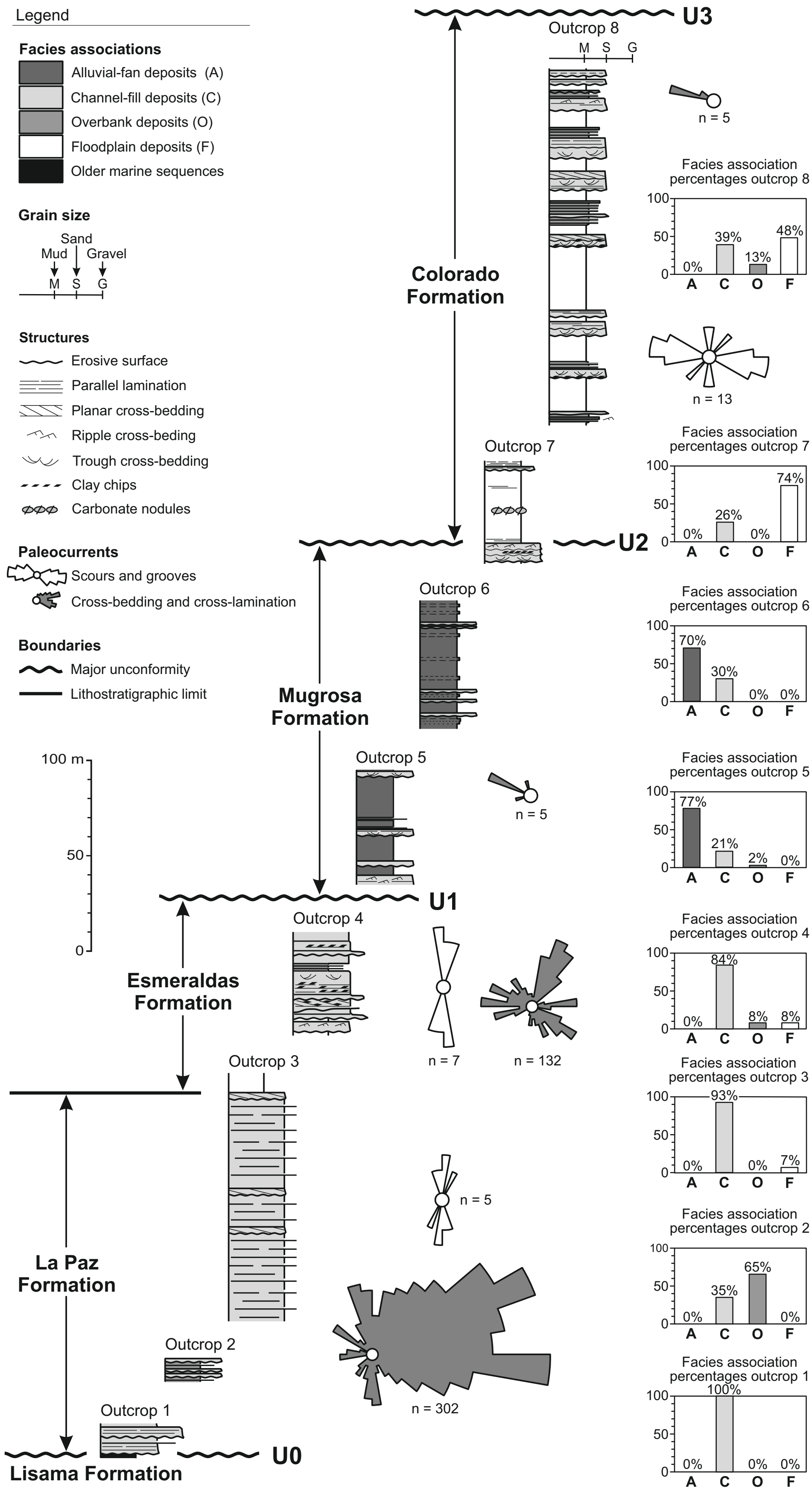

Legend
Facies associations
Alluvial-fan deposits (A)
Channel-fill deposits (C)
Overbank deposits (O)
Floodplain deposits (F)
Older marine sequences
Grain size
Sand
Mud
Gravel
M S G
Structures
Erosive surface
Parallel lamination
Planar cross-bedding
Ripple cross-beding
Trough cross-bedding
Clay chips
Carbonate nodules
Paleocurrents
Scours and grooves
Cross-bedding and cross-lamination
Boundaries
Major unconformity
Lithostratigraphic limit
100 m
50
0
U3
U2
U1
U0
Outcrop 8
Outcrop 7
Outcrop 6
Outcrop 5
Outcrop 4
Outcrop 3
Outcrop 2
Outcrop 1
Colorado Formation
Mugrosa Formation
Esmeraldas Formation
La Paz Formation
Lisama Formation
n = 5
n = 13
n = 5
n = 7
n = 132
n = 5
n = 302
Facies association percentages outcrop 8
0% 39% 13% 48%
Facies association percentages outcrop 7
0% 26% 0% 74%
Facies association percentages outcrop 6
70% 30% 0% 0%
Facies association percentages outcrop 5
77% 21% 2% 0%
Facies association percentages outcrop 4
0% 84% 8% 8%
Facies association percentages outcrop 3
0% 93% 0% 7%
Facies association percentages outcrop 2
0% 35% 65% 0%
Facies association percentages outcrop 1
0% 100% 0% 0%
A C O F
100 50 0

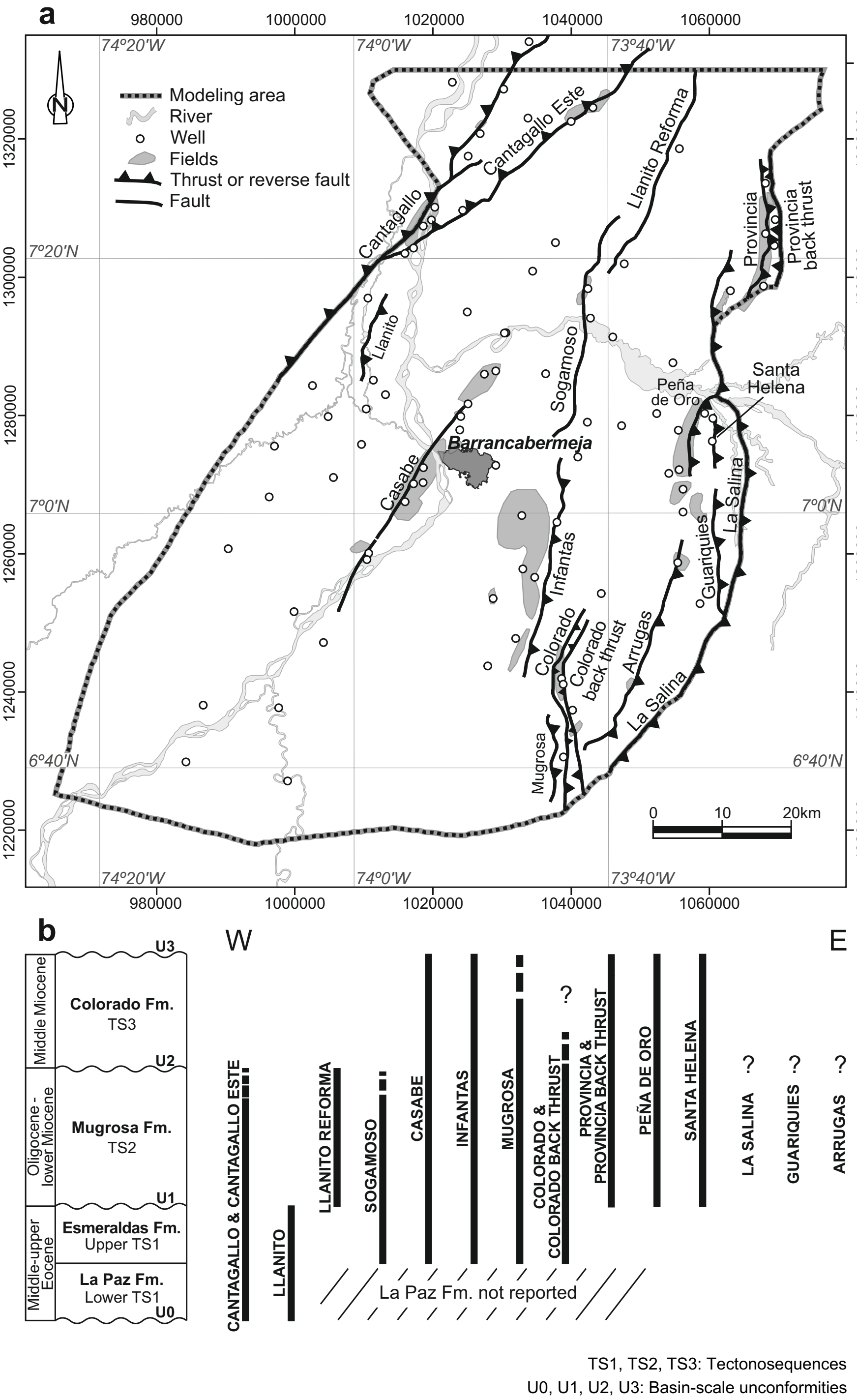
a
980000
1000000
1020000
1040000
1060000
74°20'W
74°0'W
73°40'W
7°20'N
7°0'N
6°40'N
1320000
1300000
1280000
1260000
1240000
1220000
Modeling area
River
Well
Fields
Thrust or reverse fault
Fault
N
Cantagallo
Cantagallo Este
Llanito Reforma
Provincia
Provincia back thrust
Llanito
Sogamoso
Santa Helena
Peña de Oro
Barrancabermeja
Casabe
Infantas
La Salina
Guariquies
Colorado
Colorado back thrust
Arrugas
Mugrosa
0
10
20km
b
W
E
U3
Middle Miocene
Colorado Fm.
TS3
U2
Oligocene - lower Miocene
Mugrosa Fm.
TS2
U1
Middle-upper Eocene
Esmeraldas Fm.
Upper TS1
La Paz Fm.
Lower TS1
U0
CANTAGALLO & CANTAGALLO ESTE
LLANITO
LLANITO REFORMA
SOGAMOSO
CASABE
INFANTAS
MUGROSA
COLORADO & COLORADO BACK THRUST
PROVINCIA & PROVINCIA BACK THRUST
PEÑA DE ORO
SANTA HELENA
LA SALINA
GUARIQUIES
ARRUGAS
?
La Paz Fm. not reported
TS1, TS2, TS3: Tectonosequences
U0, U1, U2, U3: Basin-scale unconformities

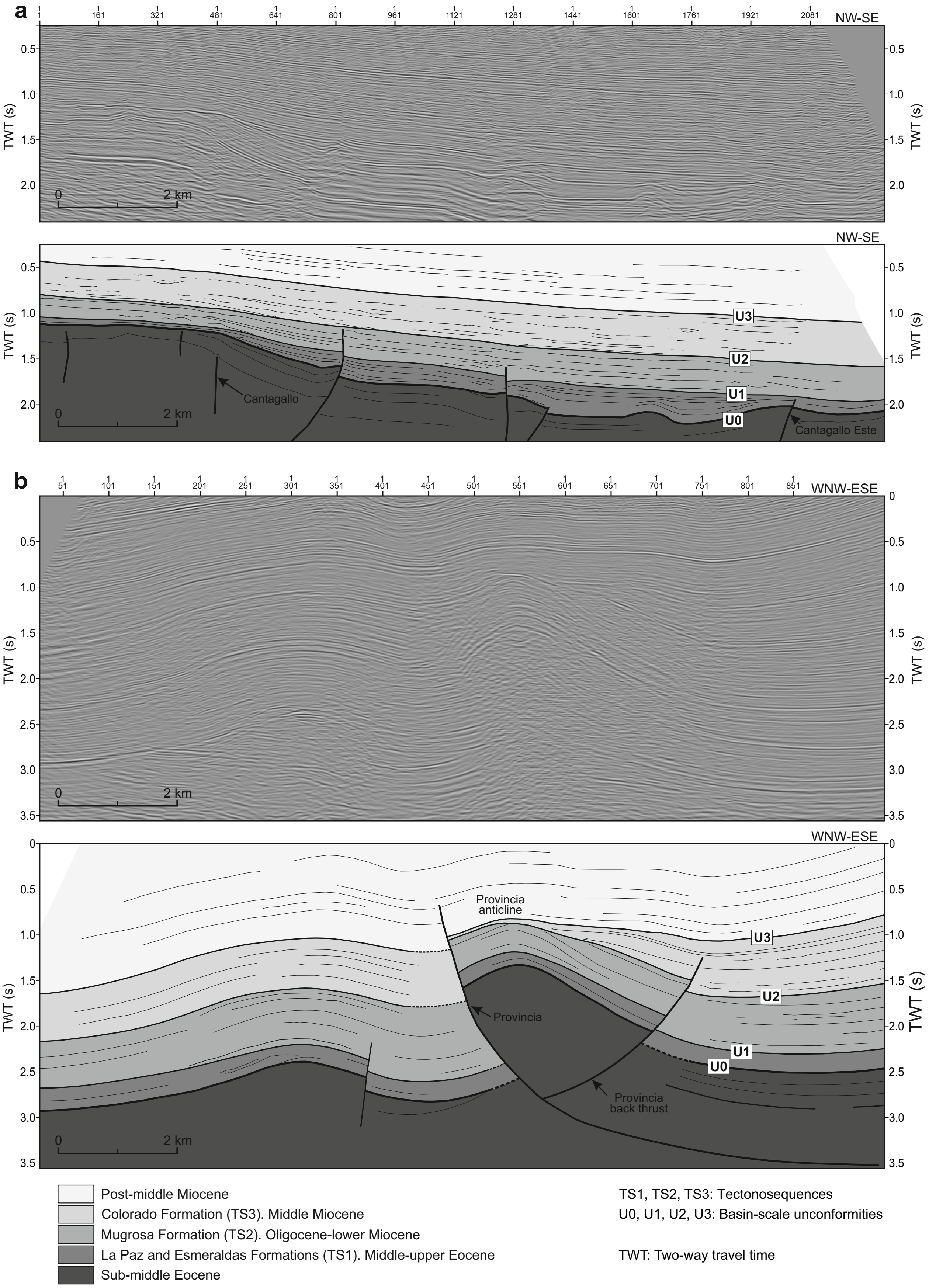

a
NW-SE
TWT (s)
0
2 km
U3
U2
U1
U0
Cantagallo
Cantagallo Este
b
WNW-ESE
Provincia anticline
Provincia
Provincia back thrust
Post-middle Miocene
Colorado Formation (TS3). Middle Miocene
Mugrosa Formation (TS2). Oligocene-lower Miocene
La Paz and Esmeraldas Formations (TS1). Middle-upper Eocene
Sub-middle Eocene
TS1, TS2, TS3: Tectonosequences
U0, U1, U2, U3: Basin-scale unconformities
TWT: Two-way travel time

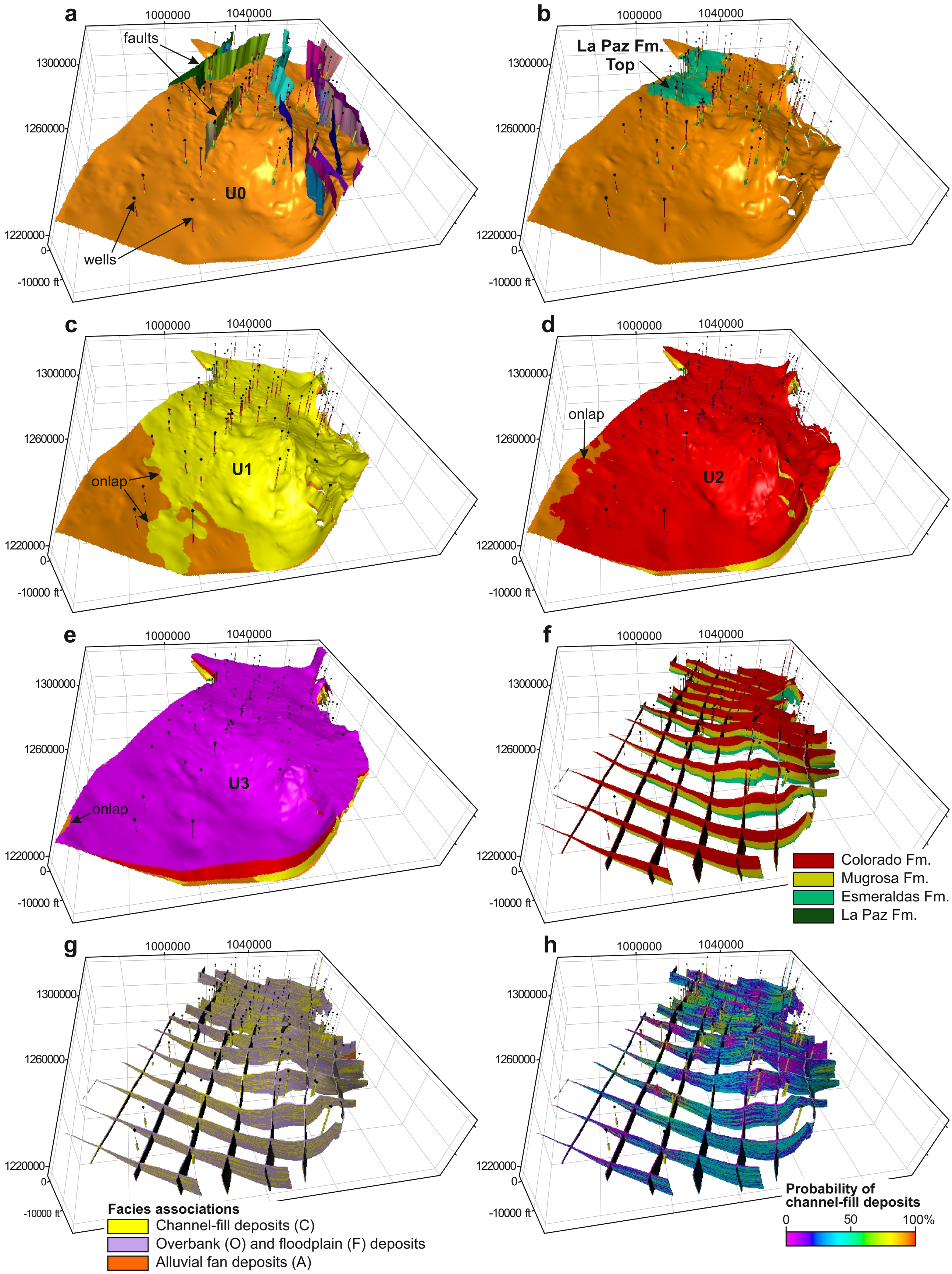

a
1000000
1040000
1300000
1260000
1220000
0
-10000 ft
faults
U0
wells
b
La Paz Fm.
Top
c
onlap
U1
d
onlap
U2
e
onlap
U3
f
Colorado Fm.
Mugrosa Fm.
Esmeraldas Fm.
La Paz Fm.
g
Facies associations
Channel-fill deposits (C)
Overbank (O) and floodplain (F) deposits
Alluvial fan deposits (A)
h
Probability of
channel-fill deposits
0
50
100%

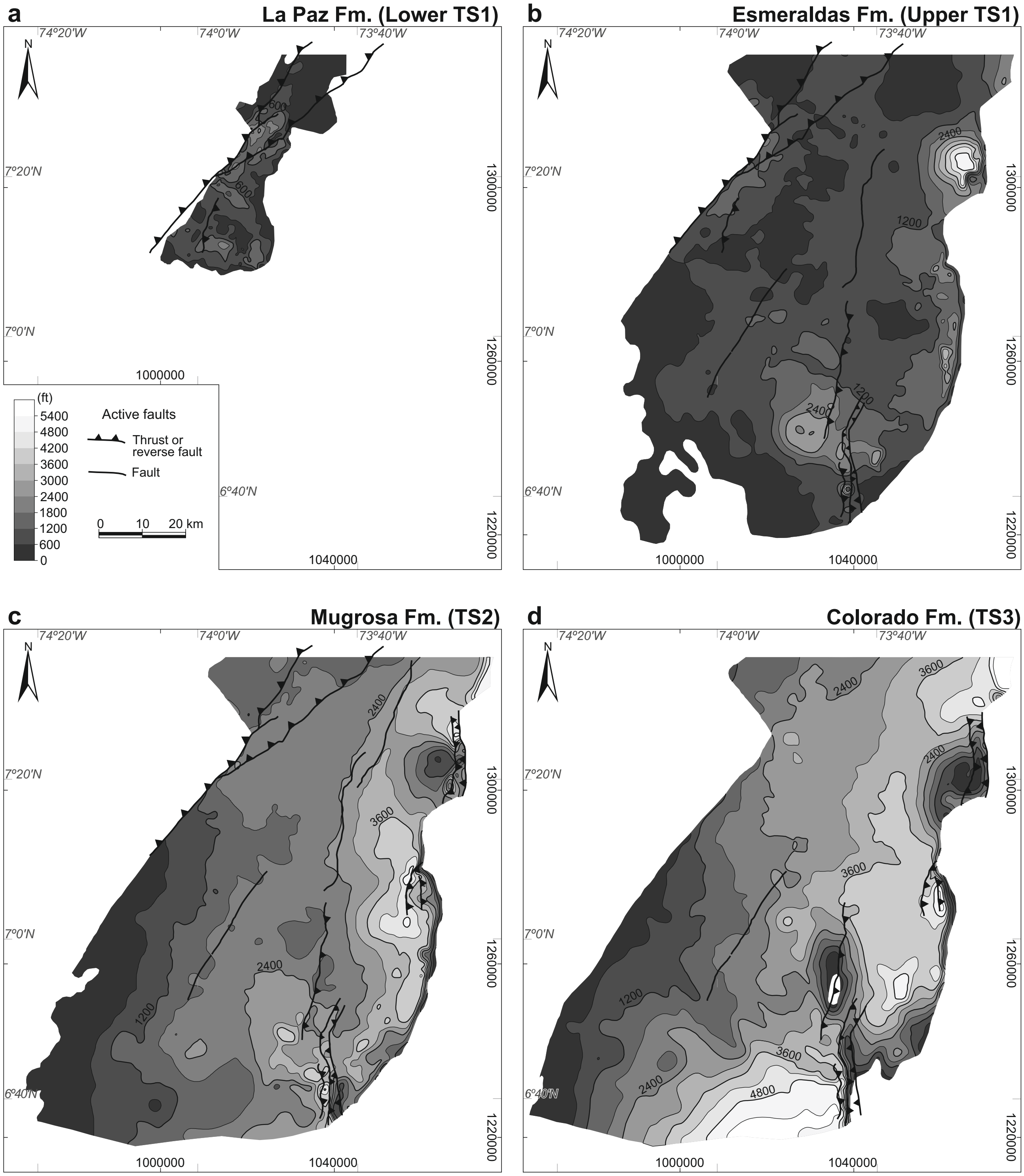
a
La Paz Fm. (Lower TS1)
b
Esmeraldas Fm. (Upper TS1)
c
Mugrosa Fm. (TS2)
d
Colorado Fm. (TS3)
N
74º20'W
74º0'W
73º40'W
7º20'N
7º0'N
6º40'N
1000000
1040000
1300000
1260000
1220000
(ft)
5400
4800
4200
3600
3000
2400
1800
1200
600
0
Active faults
Thrust or reverse fault
Fault
0
10
20 km
600
1200
2400
3600
4800

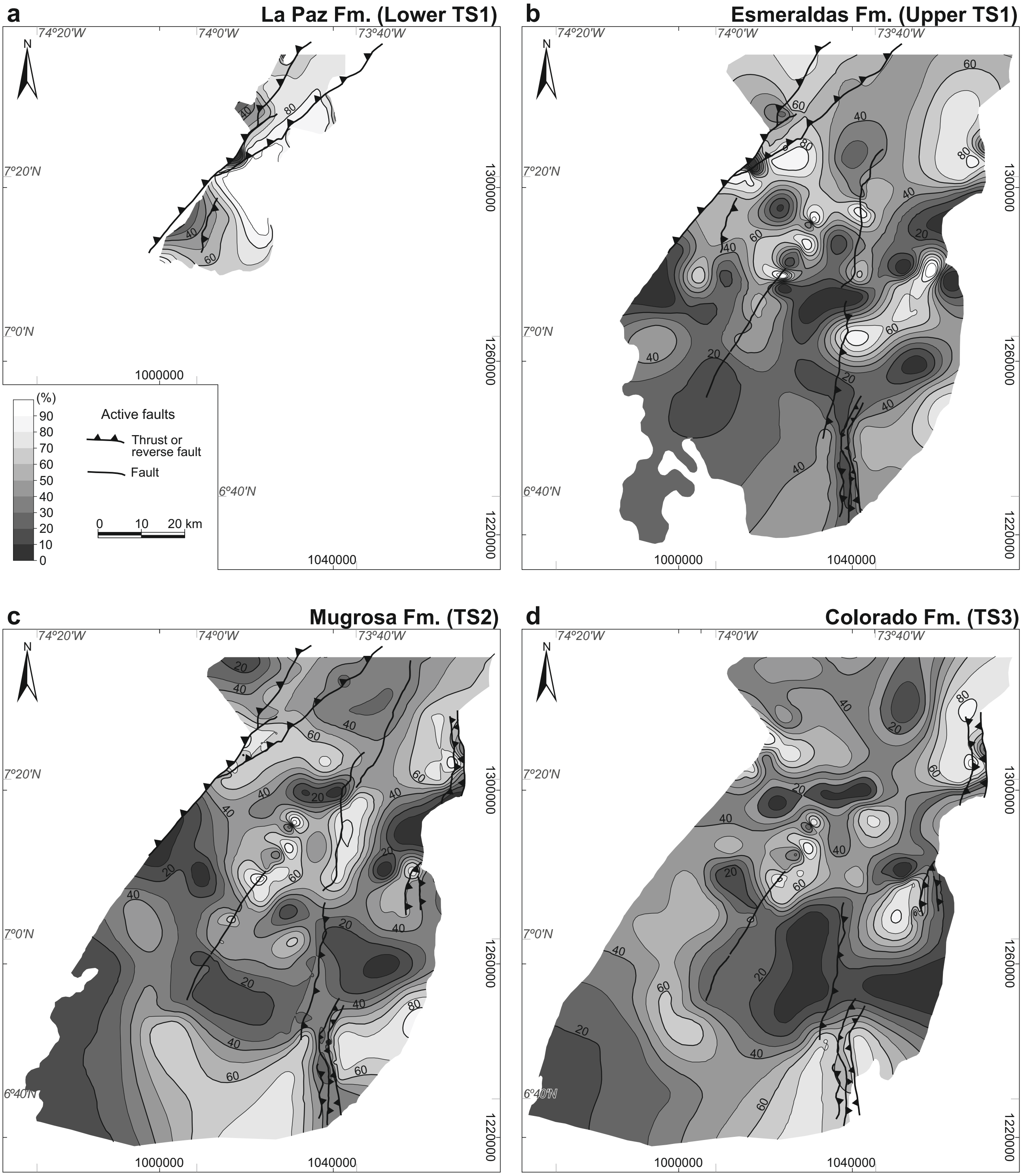
a
La Paz Fm. (Lower TS1)
74°20'W
74°0'W
73°40'W
7°20'N
7°0'N
6°40'N
1000000
1040000
1300000
1260000
1220000
N
40
80
60
(%)
90
80
70
60
50
40
30
20
10
0
Active faults
Thrust or reverse fault
Fault
0
10
20 km
b
Esmeraldas Fm. (Upper TS1)
c
Mugrosa Fm. (TS2)
d
Colorado Fm. (TS3)

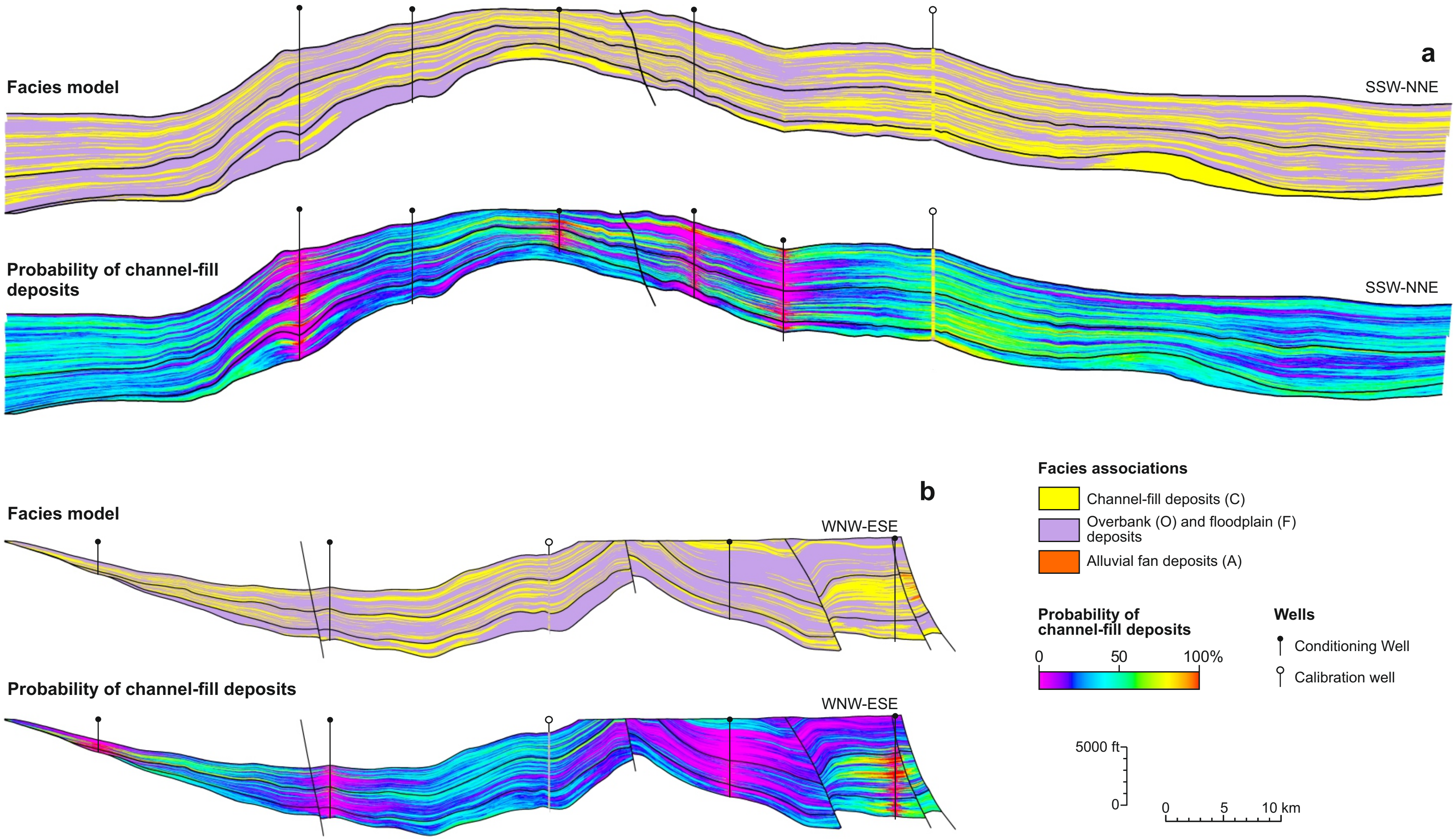

a
Facies model
SSW-NNE
Probability of channel-fill deposits
SSW-NNE
b
Facies model
WNW-ESE
Probability of channel-fill deposits
WNW-ESE
Facies associations
Channel-fill deposits (C)
Overbank (O) and floodplain (F) deposits
Alluvial fan deposits (A)
Probability of channel-fill deposits
0
50
100%
Wells
Conditioning Well
Calibration well
5000 ft
0
0
5
10 km

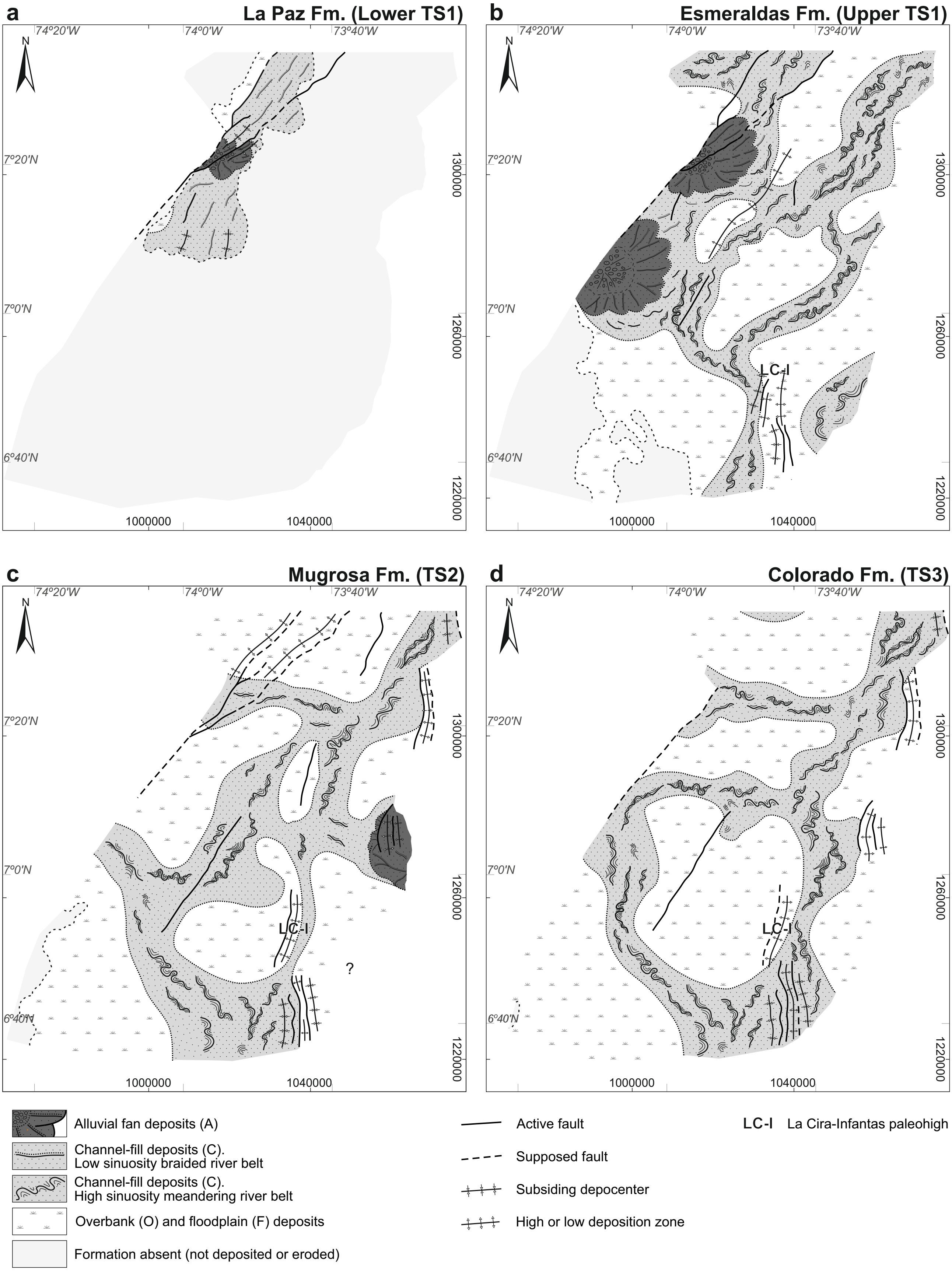
a
La Paz Fm. (Lower TS1)
b
Esmeraldas Fm. (Upper TS1)
c
Mugrosa Fm. (TS2)
d
Colorado Fm. (TS3)
N
74°20'W
74°0'W
73°40'W
7°20'N
7°0'N
6°40'N
1000000
1040000
1300000
1260000
1220000
LC-I
?
Alluvial fan deposits (A)
Channel-fill deposits (C).
Low sinuosity braided river belt
Channel-fill deposits (C).
High sinuosity meandering river belt
Overbank (O) and floodplain (F) deposits
Formation absent (not deposited or eroded)
Active fault
Supposed fault
Subsiding depocenter
High or low deposition zone
LC-I La Cira-Infantas paleohigh

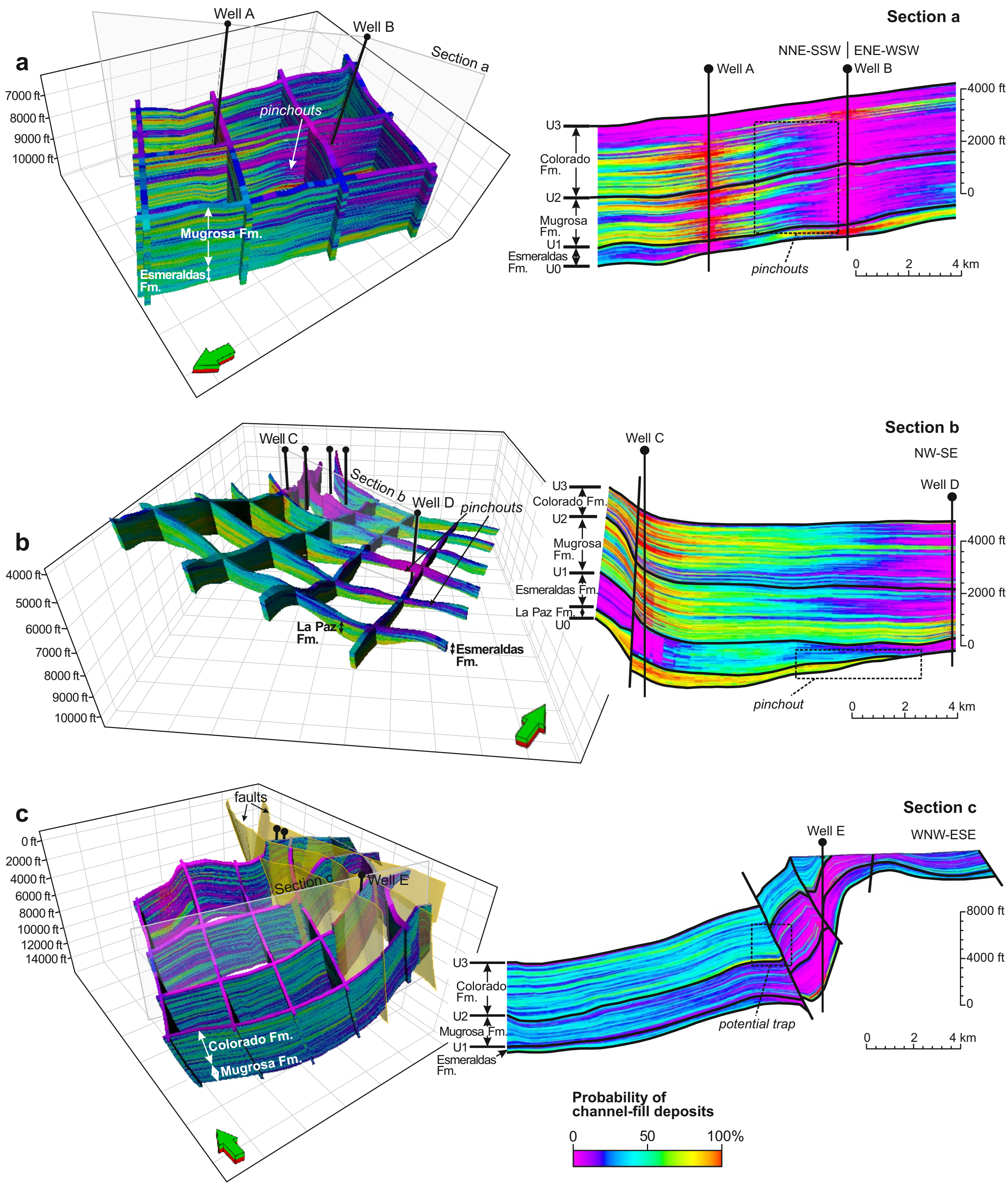
a
Well A
Well B
Section a
7000 ft
8000 ft
9000 ft
10000 ft
pinchouts
Mugrosa Fm.
Esmeraldas Fm.
Section a
NNE-SSW | ENE-WSW
Well A
Well B
U3
Colorado Fm.
U2
Mugrosa Fm.
U1
Esmeraldas Fm.
U0
pinchouts
4000 ft
2000 ft
0
0 2 4 km
b
Well C
Section b
Well D
pinchouts
4000 ft
5000 ft
6000 ft
7000 ft
8000 ft
9000 ft
10000 ft
La Paz Fm.
Esmeraldas Fm.
Section b
NW-SE
Well C
Well D
U3
Colorado Fm.
U2
Mugrosa Fm.
U1
Esmeraldas Fm.
La Paz Fm.
U0
pinchout
4000 ft
2000 ft
0
0 2 4 km
c
faults
0 ft
2000 ft
4000 ft
6000 ft
8000 ft
10000 ft
12000 ft
14000 ft
Section c
Well E
Colorado Fm.
Mugrosa Fm.
Section c
WNW-ESE
Well E
U3
Colorado Fm.
U2
Mugrosa Fm.
U1
Esmeraldas Fm.
potential trap
8000 ft
4000 ft
0
0 2 4 km
Probability of channel-fill deposits
0 50 100%

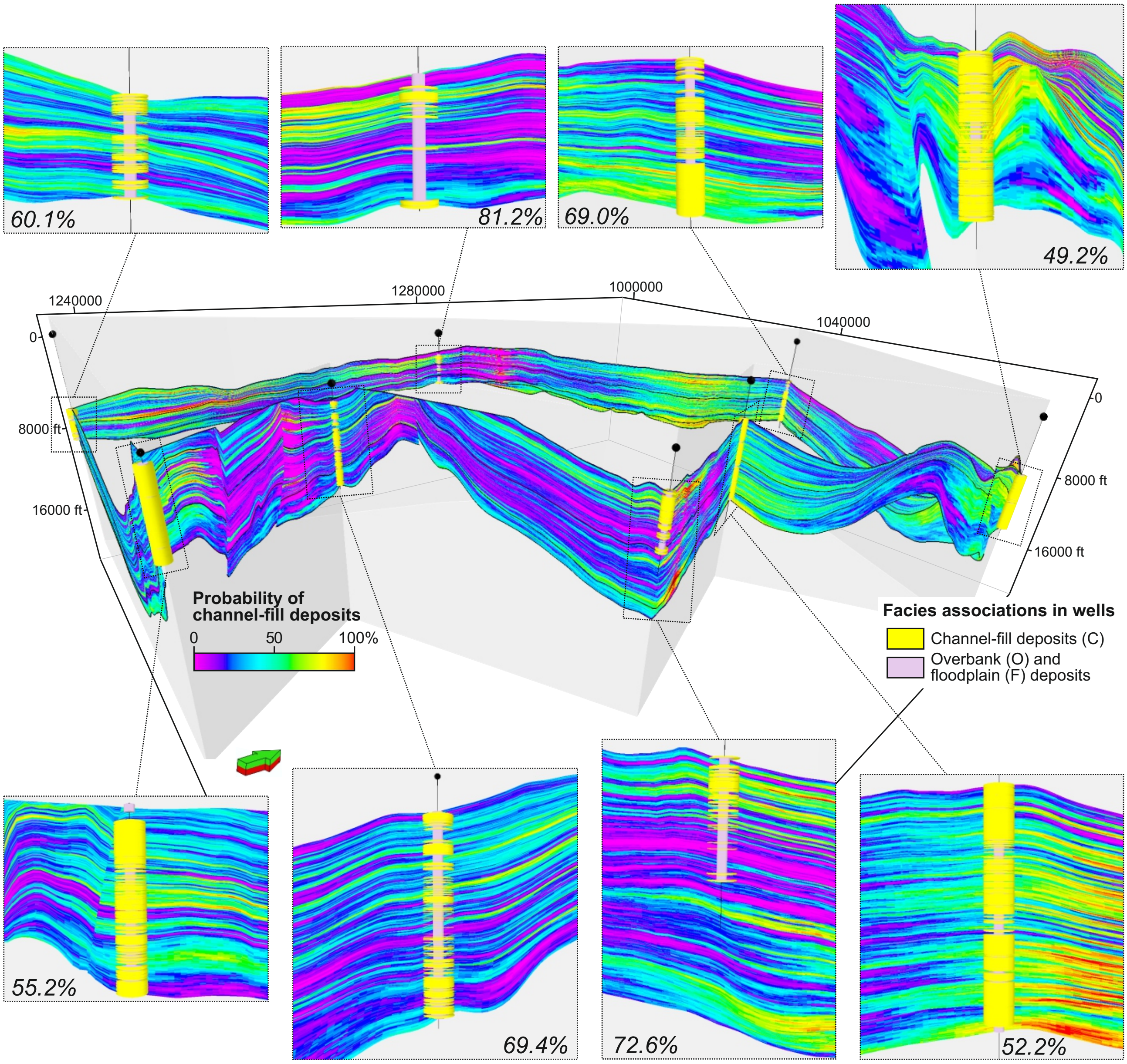

60.1%
81.2%
69.0%
49.2%
1240000
1280000
1000000
1040000
0
8000 ft
16000 ft
0
8000 ft
16000 ft
Probability of
channel-fill deposits
0
50
100%
Facies associations in wells
Channel-fill deposits (C)
Overbank (O) and
floodplain (F) deposits
55.2%
69.4%
72.6%
52.2%